

Puncture Reversal of Ethylene Ionomers – Mechanistic Studies
Rebecca Fall

Thesis submitted to the faculty of Virginia Polytechnic Institute and State University in partial fulfillment of the requirements for the degree of

Masters of Science
In
Chemistry

Dr. Thomas Ward, Chairman
Dr. John Dillard, Co-Chairman
Dr. Terry St.Clair

August 29, 2001
Blacksburg, Virginia

Keywords: ionomer, poly(ethylene-co-methacrylic acid), EMAA, Surlyn[®]

Copyright 2001, Rebecca Fall

Puncture Reversal in Ethylene Ionomers – Mechanistic Studies

Rebecca Fall

(ABSTRACT)

Ionomers are polymers that contain ionic groups in relatively low concentrations along the polymer backbone. These ionic groups, in the presence of oppositely charged ions, form aggregates that lead to novel physical properties of the polymer. React-A-Seal[®] and Surlyn[®] are poly(ethylene-co-methacrylic acid) (EMAA) ionomer-based materials and Nucrel[®] is the EMMA acid copolymer neutralized to produce Surlyn[®]. React-A-Seal[®], Surlyn[®], and Nucrel[®] recover into their original shapes following a high impact puncture at velocities ranging from 300 to 1200 ft/s ("self-healing"). This self-healing process may be of great benefit in space applications where structures are exposed to matter impacts. A thermal IR camera indicated a temperature increase to 98°C for Nucrel[®] 925, Surlyn[®] 8940, React-A-Seal[®], and Surlyn[®] 8920 after initial penetration. To understand and generalize the observed phenomena, questions concerning the mechanism of the puncture resealing must be answered. One suggestion is that the elastic character of the melt created by the puncture drives the self-healing. This inference is based on the observed temperature rise of ~3°C above the melting temperature of the samples (~95°C) during the impact.

With the expectation of gaining additional insight into the self-healing phenomenon, a thermodynamic and viscoelastic investigation was conducted using primarily DSC and DMA. Surlyn[®] and React-A-Seal[®] showed the characteristic order-disorder transition at ~52°C that has been reported in literature. Master curves were constructed from the creep isotherms for the four EMMA samples. An aging study was performed to investigate the irreproducibility and "tailing effect" observed in the creep data. The aging study indicated that, with increased aging time and temperature, changes in the polyethylene matrix lead to complexities in morphology resulting in changes in the magnitude and shape of the creep curves.

As a result of the thermodynamic, viscoelastic, and high-speed impact experiments it has been theorized that self-healing can occur in Nucrel[®] 925, Surlyn[®] 8940, React-A-Seal[®], and Surlyn[®] 8920 because of two features, ionic aggregation and complex flow behavior.

Acknowledgments

Many people have helped make this endeavor a success. I would like to thank the following people for their guidance and support.

Dr. Dave Dillard, Center for Adhesive and Sealant Science, encouraged me to pursue a graduate degree and supported my decisions. Without him I may not have met Dr. Terry St.Clair at NASA-LaRC.

Dr. Terry St.Clair assisted me in obtaining funding through NASA and presented me with a potential project; he was a primary motivation for pursuing this masters. He also graciously agreed to serve on my committee. I am very grateful and appreciative for all he has done.

Dr. Tom Ward and Dr. John Dillard for agreeing to advise me and supporting my proposed timeline.

Individuals at NASA-LaRC – Paul Bagby, Norman McRea, Bud Schuszler, Joel Aleska, Erik Weiser, and Sean Britton.

A special thanks goes to Bob Berry and Crystal Topping. They were great friends and always did whatever they could to help me attain my goals.

Members of the PolyPkem research group – Sandra Henderson, Catherine Beck, Amy Eichstadt, Emmett O'Brien, and Jennifer Robertson – for their advice and assistance. They helped make each day enjoyable and passed on valuable knowledge.

Tammy Jo Hiner, Millie Ryan, and Esther Brann for their assistance and useful advice.

Finally, I would like to thank my family, my Mom and Dad for their never-ending encouragement, support, and love; my sister and brother for their love and motivation; and John for making me laugh and encouraging me to pursue my dreams.

Table of Contents

1.	Literature Review.....	1
1.1.	Introduction.....	1
1.2.	Ionomers.....	2
1.2.1.	Definition of Ionomer.....	2
1.2.2.	Composition of an Ionomer.....	2
1.3.	Ionic Aggregate Formation.....	2
1.3.1.	Multiplets.....	2
1.3.2.	EHM Model.....	3
1.4.	Influence of Aggregate Formation on Thermal, Mechanical, and Physical Properties.....	5
1.4.1.	Differential Scanning Calorimetry (DSC) Background.....	5
1.4.1.1.	Order-Disorder Transition.....	7
1.4.2.	Dynamic Mechanical Analyzer (DMA) Background.....	9
1.4.2.1.	Modulus Trends.....	11
1.4.3.	Rheometer Background.....	14
1.4.3.1.	Viscosity.....	15
1.5.	Thermoplastic Ionomers.....	16
1.5.1.	Nucrel [®] 925.....	16
1.5.2.	Surlyn [®]	17
1.5.3.	React-A-Seal.....	18
1.6.	References.....	18
2.	Experimental.....	20
2.1.	Materials.....	20
2.2.	XPS.....	20
2.3.	TGA.....	20
2.4.	DSC.....	20
2.5.	Compression Molding.....	21
2.6.	Pistol Range High-Speed Impact Studies.....	21

2.7.	DMA.....	23
2.8.	Rheometer.....	23
3.	Results and Discussion	
	Physical, Thermal, and Mechanical Characterization.....	24
3.1.	XPS of React-A-Seal.....	24
3.2.	TGA.....	26
3.3.	DSC.....	28
3.4.	DMA.....	30
3.5.	References.....	35
4.	Results and Discussion	
	Viscoelastic Characterization.....	37
4.1.	DMA.....	37
	4.1.1. DSC Aging	48
4.2.	Summary.....	53
4.3.	References.....	53
5.	Results and Discussion	
	High-Impact Projectile Testing.....	55
5.1.	Pistol Range.....	55
	5.1.1. Thermal IR Camera.....	57
	5.1.2. Rheometer.....	59
5.2.	References.....	61
6.	Comments on the Self-Healing Phenomenon.....	62
7.	Future Work.....	63

List of Figures

Figure 1.1 A multiplet in poly(S-co-MANa) ionomer which illustrates a region of restricted mobility.....	4
Figure 1.2 Morphological representations of random ionomers under various ionic conditions.....	5
Figure 1.3 Ideal DMA curve with labeled characteristics.....	6
Figure 1.4. DSC curves for EMAA-0.6Zn-0.97BAC; 1H, first heating; 1C, first cooling; 2H, second heating; second heating processes after storing for (A) 5h, (b) 1 day, (c) 3 days, (d) 9 days, and (e) 38 days at room temperature.....	7
Figure 1.5. Model for the order-disorder transition of the ionic clusters.....	8
Figure 1.6. DSC curves for E-0.133MAA-0.6Na; 1H, first heating; 1C, first cooling; 2H, second heating immediately after the 1C scan; 2H scans after storing for (a) 5h, (b) 1 day, (c) 3 days, (d) 9 days, and (e) 38 days at room temperature.....	9
Figure 1.7. Illustration of creep and creep recovery.....	10
Figure 1.8. Temperature dependence of dynamic storage modulus (E') and loss modulus (E'') at 10 Hz for sodium salts of EMAA ionomers.....	12
Figure 1.9. Temperature dependence of the dynamic loss modulus (E'') at 1, 10, 100 Hz frequencies for EMAA-0.9Zn.....	13
Figure 1.10. Diagram showing the regions of flow behavior, both Newtonian and non-Newtonian.....	14
Figure 1.11. Schematic illustrating the “ion hopping” relaxation mechanism in ionomers	15
Figure 1.12. EMAA polymer with the acid group (outlined in red).....	17
Figure 1.13. EMAA – neutralized with sodium (outlined in red).....	17
Figure 2.1. Schematic of range setup.....	22
Figure 2.2. (a) Shows a standard 9mm bullet, (b) shows a “polish” 9-mm bullet.....	22

Figure 3.1. Structure of methacrylic acid.....	25
Figure 3.2. Curve-fit for the C 1s and O 1s peaks from XPS narrow scan.....	25
Figure 3.3. Graph of weight percent versus temperature.....	27
Figure 3.4. First heat (1H) and second heat (2H) for the Nucrel [®] 925, Surlyn [®] 8940, React-A-Seal [®] , and Surlyn [®] 8920 from the DSC.....	29
Figure 3.5. Temperature dependence of dynamic loss modulus (E'') at (a) 1 Hz, (b) 10 Hz, and (c) 100 Hz – The α , α' , β , and β' designations are a result of the Arrhenius analysis.....	32
Figure 3.6. An Arrhenius plot for the α relaxation in React-A-Seal [®]	33
Figure 4.1. Schematic of the compression geometry - the amount of penetration by the probe is dictated by the temperature and stress applied in the experiment.....	37
Figure 4.2. (a) Creep isotherms at 1.5 MPa stress and (b) creep recovery isotherms at 0 MPa stress for Nucrel [®] 925 at temperatures between 30°C and 79°C.....	38
Figure 4.3. (a) Creep isotherms at 1.5 MPa stress and (b) creep recovery isotherms at 0 MPa stress for Surlyn [®] 8940 at temperatures between 30°C and 82°C.....	39
Figure 4.4. (a) Creep isotherms at 1.5 MPa stress and (b) creep recovery isotherms at 0 MPa stress for React-A-Seal [®] at temperatures between 30°C and 82°C.....	40
Figure 4.5. (a) Creep isotherms at 1.5 MPa stress and (b) creep recovery isotherms at 0 MPa stress for Surlyn [®] 8920 at temperatures between 30°C and 82°C.....	41
Figure 4.6. (a) tTSP master curve and (b) shift factor plot for Nucrel [®] 925.....	43
Figure 4.7. (a) tTSP master curve and (b) shift factor plot for Surlyn [®] 8940.....	44
Figure 4.8. (a) tTSP master curve and (b) shift factor plot for React-A-Seal [®]	45
Figure 4.9. (a) tTSP master curve and (b) shift factor plot for Surlyn [®] 8920.....	46
Figure 4.10. Aging of Nucrel [®] 925 for 30 minutes in the DSC from 30°C to 90°C.....	48
Figure 4.11. Aging of Surlyn [®] 8940 for 30 minutes in the DSC from 30°C to 90°C.....	49
Figure 4.12. Aging of React-A-Seal [®] for 30 minutes in the DSC from 30°C to 90°C.....	49
Figure 4.13. Aging of Surlyn [®] 8920 for 30 minutes in the DSC from 30°C to 80°C.....	50
Figure 5.1. Sample of React-A-Seal [®] (a) healed after high-speed impact with standard 9mm bullet, (b) un-healed after high-speed impact with “polish” bullet.....	55

Figure 5.2. Schematic showing the ordering and disordering of an ionic aggregate with heat as the source of energy57

Figure 5.3. A thermal IR image from React-A-Seal®58

Figure 5.4. Graph of viscosity as a function of shear rate for Nucrel® 925, Surlyn® 8940, React-A-Seal®, and Surlyn® 8920 at 90, 110, 130, and 150°C.....60

List of Tables

Table 3.1 Data from React-A-Seal [®] XPS spectrum.....	24
Table 3.2 Peak assignments for C 1s and O 1s from the curve-fit narrow scan.....	25
Table 3.3 Degradation temperatures for each sample at 2, 5, 10, and 95% weight loss.....	25
Table 3.4 Data from XPS spectra of Surlyn [®] 8940, React-A-Seal [®] and Surlyn [®] 8920 TGA pan residue.....	28
Table 3.5 Maximum temperature of order-disorder transition.....	29
Table 3.6 Activation energies for the relaxations of each sample with peak designations	33
Table 3.7 Comparison of the measured temperatures of the order-disorder transition in the DSC and the temperature of the highest temperature relaxation from the loss modulus curve in Figure 3.4.....	35
Table 4.1 Comparison of the order-disorder transition temperatures from the DSC, DMA frequency dependent data, and the DMA creep data.....	47
Table 4.2 Comparison of the peak maximum and percent crystallinity for the quasi-crystalline peak for each sample and percent crystallinity for the melting peak for each sample.....	51
Table 5.1 Data for React-A-Seal [®] showing the changes in temperature of the sample with impact of a 9-mm bullet and the changes in velocity of the bullet upon impact.....	58
Table 5.2 Provides the maximum strain rates reached at the maximum stresses measured for the ionomer samples.....	61

1. Literature Review

1.1. Introduction

Ionomers of all types, whether based on styrene, ethylene, butadiene, urethane or sulfones, have been used for successful industrial applications. These applications include using ionomers as membranes or thin films, in fuel cells, packaging, coatings in the fertilizer industry, floor polishes, and adhesives. The addition of the ionic character to a polymer enhances the physical characteristics and strongly influences the glass transition temperature, modulus, viscosity, and optical features resulting in the improvement of physical and mechanical behavior. The coulombic interactions due to ionic groups play a major role in contributing to such properties as high tear resistance, toughness, flexibility, melt strength, and the use of ionomers as additives for the purpose of enhancing miscibility.

For 30 years scientists have been studying ionomers both microscopically and macroscopically. A modest fundamental understanding has been established, yet much still remains to be learned about the novel properties of ionomers. Considerable controversy surrounds issues like the morphology of ionic aggregates and their physical behavior. Finding a relationship between chemical structure, morphology, and physical properties presents difficult problems and potential prospects for discovery to both academia and industry. The investigation of property changes, which occur due to ionic aggregation, is of primary importance to the study of ionomers.

Remarkably, it has been speculated that these ionic interactions aid in the ability of poly(ethylene-co-methacrylic acid) – Na⁺ ionomers to self-heal following high-speed impact. An attempt to understand this phenomenon is the focus of the current research. It is hoped that these “smart” materials might have applications in space; primarily for protecting the space station or space shuttle from destructive micrometeorite impacts. Currently, the poly(ethylene-co-methacrylic acid) ionomers with self-healing properties are not space compatible; the ionomers are not resistant to UV or atomic oxygen degradation. With an understanding of why this healing phenomenon occurs, ionomers could be synthesized or modified, e.g. by fillers, to be space compatible and able to self-heal upon impact.

1.2. Ionomers

1.2.1. Definition of Ionomer

In 1965, Rees and Vaughan defined ionomers as olefin-based polymers containing a relatively small percentage of ionic groups in which “strong ionic interchain forces play the dominant role in controlling properties”.¹ With time, as new polymer backbones and more ionic character were being incorporated into ionomers, it was recognized that there were problems with this definition. These new ionomers behaved very similarly to polyelectrolytes, especially in solvents with high dielectric constants. This confusion between polyelectrolytes and ionomers led to a new definition by Eisenburg and Rinaudo in 1990². The new definition stated that ionomers are “polymers in which the bulk properties are governed by ionic interactions in discrete regions of the material (ionic aggregates)”, specifically in materials where the ion content is less than about 15 mol %. This new definition now attributed the behavior of ionomers to their properties rather than their composition, thereby differentiating an ionomer from a polyelectrolyte.

1.2.2. Composition of an Ionomer

Typically, ionomers are low dielectric copolymers comprised of nonionic repeat units and ionic repeat units. Alkali metals and alkaline earth metals, for example, act as counter ions for these acid (anionic) polymers. Distribution of these ionic groups along the backbone chain is an important variable. The ionic groups can be synthetically placed randomly or systematically within the primary polymer chain (e.g. ionenes), as end groups on polymer chains (e.g. monochelics, telechelics), or as segments in a block copolymer.^{3,4} Regardless of the ionic group placement, the groups facilitate the formation of ionic aggregates. The ionic aggregates are effectively physical crosslinks, which give rise to ionomers with thermoplastic characteristics.

1.3. Ionic Aggregate Formation

1.3.1. Multiplets.

Ion – counter ion and ion pair – ion pair associations strongly drive the formation of multiplets, the smallest form of an ionic aggregate³. With the assumption, initiated by Li *et al.*⁵,

that multiplets are nearly spherical in shape, it has been estimated by Eisenburg³ that less than approximately 10 ion pairs aggregate to form a multiplet. The size of the multiplet not only depends on the shape, but also on the size of the ion pair, the size of the chain segment in contact with the ion, the distance between the ion pairs, and the electrostatic energy between the ion pairs.

Spatial arrangements of multiplets have been investigated experimentally and theoretically since the late 1960s, beginning with small angle x-ray scattering (SAXS) studies conducted by Wilson *et al.*⁶ and Longworth and Vaughan⁷. They found that an ionic peak could be detected in ethylene ionomers at low angles. The authors linked this peak to the presence of ionic aggregation. This information was useful in the development of further models like the Multiplet-Cluster Concept^{8,9} in 1970, the Hard-Sphere Model^{10,11} in 1973 (modified in 1983), and the Core-Shell Model^{12,13} in 1974 (modified in 1980). All of these models discussed only SAXS profiles and neglected to account for the mechanical properties of the material.

1.3.2. EHM Model.

In 1990, the EHM Model³ (Figure 1.1) was developed by Eisenburg, Hird, and Moore to relate ionomer morphology to mechanical properties. In this model, as the ion content increases, the restricted mobility layer (the approximate 10Å layer of chains anchored to the multiplet) is reduced relative to the bulk material (Figure 1.1)³.

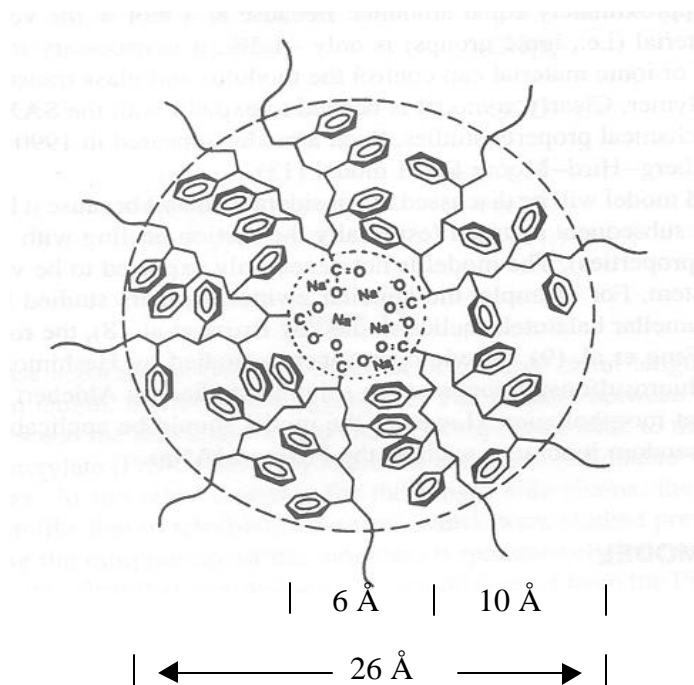


Figure 1.1. A multiplet in poly(S-co-MANa) ionomer which illustrates a region of restricted mobility³

Several factors, some more important than others, could account for the restricted mobility. First, securing a bulk chain to the multiplet essentially increases the molecular weight of the chains neighboring that multiplet, thereby causing immobilization. Second, during the formation of multiplets, electrostatic energy is released which in conjunction with surface energies results in chain crowding immediately around the multiplet. Third, chain extension can occur around the multiplet, which will allow more chains to be involved in the multiplet formation and restrict mobilization.

The glass transition temperature (T_g) is one example of a property influenced by the polymer's ionic character. As shown in Figure 1.2³, the physical property of T_g is related schematically to the amount of ion in the ionomer. The concentration of ion present dictates the extent of area with restricted mobility. At low ion content, Figure 1.2(a), no overlap of the restricted mobility regions occurs and one T_g is expected. This is because the few multiplets inter-dispersed among the bulk exhibit characteristics similar to the bulk material; the multiplets

act only as crosslinks and do not exhibit behavior independent from the bulk. For a polymer with high ion content, Figure 1.2(c), a large overlap of the restricted mobility regions is apparent and thus two T_g s are expected, one for the multiplet domains and one for the bulk behavior. The multiplets act as physical crosslinks but they also exhibit independent phase behavior - this occurs when the restricted mobility region is larger than 50-100 Å. These formations are referred to as clusters.

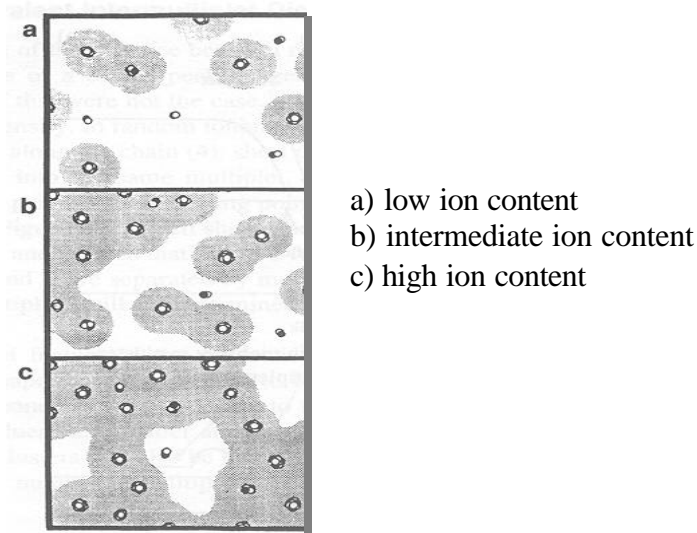


Figure 1.2. Morphological representations of random ionomers under various ionic conditions. The shaded areas represent regions of restricted mobility³.

The aggregate formations, whether multiplets or clusters, give rise to novel properties in ionomers, including changes in T_g , new thermal transitions, and higher modulus, viscosity, and melt strength. These properties can be measured with such instruments as a differential scanning calorimeter (DSC), and a dynamic mechanical analyzer (DMA). These instruments have been used to identify a new thermal transition characteristic of the aggregation in ionomers, the “order-disorder” transition.

1.4. Influence of Aggregate Formation on Thermal, Mechanical, and Physical Properties

Before discussing in detail the order-disorder transition, a basic understanding of the

DSC and the information it provides about thermal and physical changes of a polymer are needed.

1.4.1. Differential Scanning Calorimetry (DSC) Background

DSC is used to investigate thermal transitions, including phase changes, crystallization, melting, or glass-rubber transitions, of a material as a function of time and temperature. Heat flow, that is heat absorption (endothermic) or heat emission (exothermic), is measured, per unit time with the sample compared to a thermally inert reference.

The reference pan and sample pan sit on thermoelectric discs in the DSC. Thermocouples measure the temperature change between the reference material and the sample as temperature is controlled. If the sample exhibits a phase change, energy is either absorbed, or energy is emitted. In either case a change in the temperature is detected and the resulting signal is power. The plot produced from the DSC shows heat flow, the power signal, versus the temperature. Figure 1.3 shows an ideal plot from the DSC. The general transitions expected are shown, the glass transition, which is represented by a step in the endotherm, the melting of the polymer, an endothermic peak, and crystallization of the polymer, an exothermic peak.

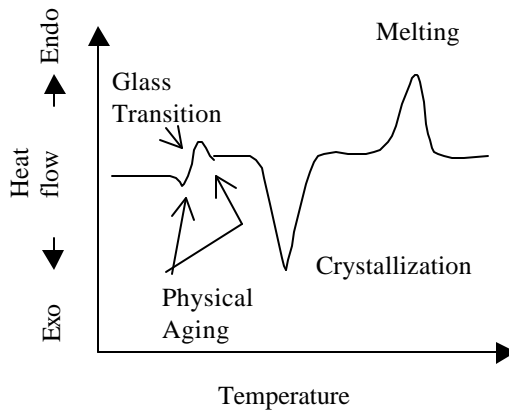


Figure 1.3. Ideal DSC curve with labeled characteristics

The DSC can also be used to investigate physical aging of glassy regions of a polymer, that is investigate the history of how the polymer was prepared and stored. Physical aging can only occur if the sample is stored or tested below its T_g . In Figure 1.3, physical aging is shown by a combination of a step in the endotherm and a peak. The area of the peak is related to how long the sample has existed in its glassy state. The placement of the peak is an artifact of

whether the sample was fast cooled and then slowly heated, or if the sample was slow cooled and then heated up quickly to afford a peak after the endotherm step. To erase the history of a polymer, the polymer can be heated above its T_g for a set amount of time. This process will give the polymer chains time to relax into a conformation where the amount of free volume is minimized. With this understanding of the DSC, the literature on the ionomer order-disorder transition can be addressed.

1.4.1.1. Order-Disorder Transition

It has been stipulated that the order-disorder transition describes the movement of the ionic aggregates from an ordered state to a disordered state as a result of temperature changes. Differential scanning calorimetry (DSC) has been used to study the order-disorder transition. In studies conducted by Tadano *et al.*^{14,15}, the order-disorder transition in poly(ethylene-co-methacrylic acid), EMAA, (5.4 mol% methacrylic acid units) - zinc neutralized ionomer system was studied. The extent of neutralization was varied and an additional component, 1,3-bis(aminomethyl)cyclohexane, was added. Using the DSC, a first and second heat was applied to the samples as presented in Figure 1.4. In the first heat, a thermal transition occurred at approximately 58°C (331K) - prior to the expected melting peak of the polyethylene matrix regions. In the first cooling scan and second heat scan (run soon after the first heat) this transition was suppressed.

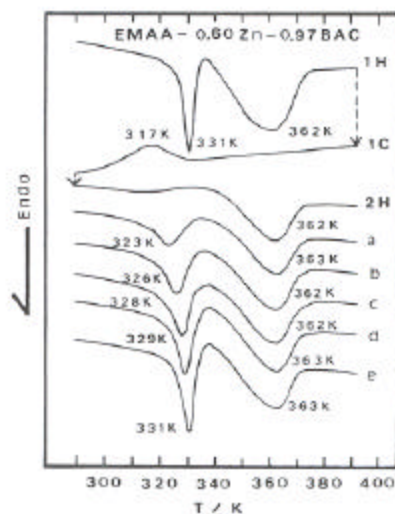


Figure 1.4. DSC curves for EMAA-0.6Zn-0.97BAC; 1H, first heating; 1C, first cooling; 2H, second heating; second heating processes after storing for (A) 5h, (b) 1 day, (c) 3 days, (d) 9 days, and (e) 38 days at room temperature¹⁴.

Tadano *et al.* observed that if, after the first cooling, the sample was stored at room temperature, the suppressed peak would return. When the sample was stored for 5 hours at room temperature, a small peak reappeared at 50°C (323 K). With increasing aging time at room temperature the peak shifted to higher temperatures and became larger. To get the suppressed peak back to its original magnitude, the samples had to be stored at room temperature for 38 days. Tadano *et al.* stipulated that this peak indicated a movement of the ionic aggregates from an ordered state, which is the configuration of the aggregates as the first heating begins, to a disordered state produced by the first heat. Figure 1.5 shows a model illustrating this order-disorder transition (T_i).

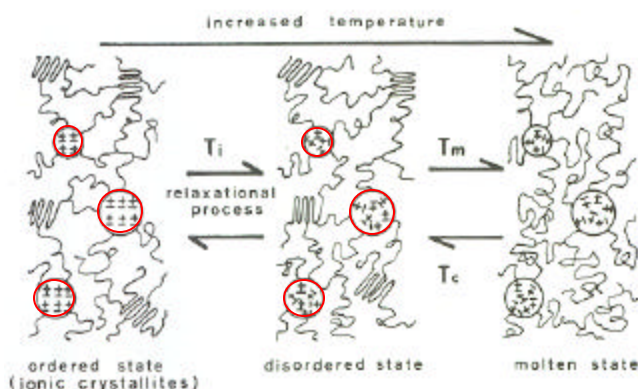


Figure 1.5. Model for the order-disorder transition of the ionic clusters¹⁵

To support this explanation, Tadano *et al.* observed that upon annealing at 23°C, the ΔH of the T_i peak increased with aging time (up to 38 days). This increase in ΔH indicated that the ionic aggregates were gradually reforming, or reordering, in a relaxation process at room temperature. To prove that the new peak was due to structural changes of the ionic aggregates, these scientists performed a series of annealing studies. These showed that the new order-disorder peak did not shift with annealing temperature, and was therefore not due to melting of quasi-crystallites in the polyethylene matrix regions.

Another study by Kutsumizu *et al.*¹⁶ reported results consistent with Tadano *et al.* for an EMAA - sodium neutralized ionomer system. In Figure 1.6, an order-disorder peak at 64°C

(337K) was suppressed after the first heat and slowly returned to its original magnitude upon aging at room temperature. Notice that the final temperature of the new order-disorder peak after 46 days of aging was at a slightly higher temperature, 70°C (343 K), versus the original peak at 64°C (337K). Kutsumizu *et al.* did not explain this observation. To continue exploring the order-disorder transition and other relaxations, an understanding of the fundamentals of the DMA is necessary.

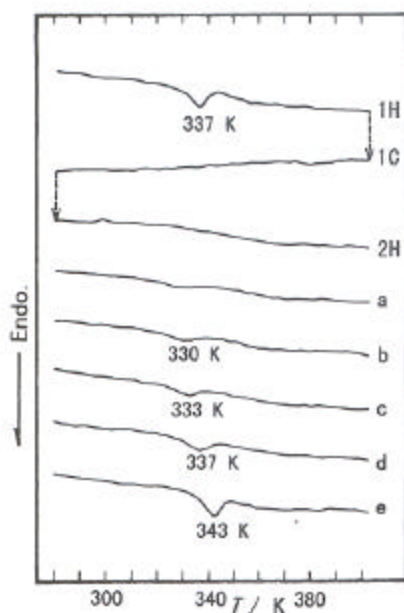


Figure 1.6. DSC curves for E-0.133MAA-0.6Na; 1H, first heating; 1C, first cooling; 2H, second heating immediately after the 1C scan; 2H scans after storing for (a) 5h, (b) 1 day, (c) 3 days, (d) 9 days, and (e) 38 days at room temperature¹⁶.

1.4.2. Dynamic Mechanical Analyzer (DMA) Background

A DMA¹⁷ is an instrument used to identify small and large-scale relaxations of materials in the solid state via an applied oscillatory stress. This is done by varying the sinusoidal stress applied to the polymer using frequency and temperature. Different geometries can be studied such as the single or double cantilever beam, tensile, or compression modes. When the stress is applied, its phase angle shift with resulting strain can be measured. The relationship between the stress and the strain is a function of the material structure and can be analyzed in terms of the storage modulus (E') and the loss modulus (E''). Each modulus can be calculated from the

measurement of the phase angle and oscillatory amplitudes as a function of time and temperature. The storage modulus for a viscoelastic polymer describes the polymer's ability to store energy upon deformation, an elastic behavior. The loss modulus is proportional to the cyclic loss of energy, a viscous behavior. $\tan \delta$ is defined as E''/E' . All of these measurements when plotted against time and temperature provide an enormous structural characterization of the polymer. From these measurements information is provided about chain motion, specifically, when the main chains begin to rotate and disentangle (T_g), and when side chain motions begin.

The DMA can also be used to measure other viscoelastic characteristics like creep and creep recovery. In this case, stress is held constant at a particular temperature, the strain changes are measured, and compliance (strain/stress) may be determined. Modulus (E) is inversely related to compliance (D), a measure of the softness of a polymer. In the creep mode, the compliance is determined as a function of time. In the creep recovery experiment, the stress is removed and compliance is again measured as time passes. This is illustrated in Figure 1.7 below.

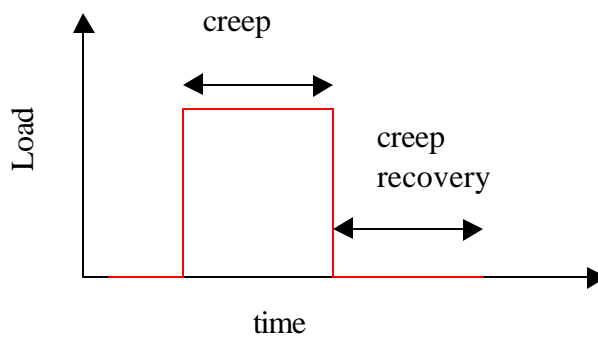


Figure 1.7. Illustration of creep and creep recovery

With either the creep/creep recovery data or the dynamic data, time-temperature superposition (tTSP) can be performed on the data to give a composite curve, known as a master curve. This master curve may be analyzed in accordance with the Williams-Landel-Ferry equation:

$$\log a_T = \frac{-C_1'(T_{ref} - T_g)}{C_2' + (T_{ref} - T_g)}$$

$\log a_T$ is the shift factor, C_1 and C_2 are constants, and T_{ref} is the temperature of the isotherm from which the remaining isotherms are shifted. If a master curve conforms to the following assumptions then it can be used to predict material properties measured at experimentally unattainable times and temperatures:

1. Over the temperature range of the original data, there is no change in the polymer parameters (chemical composition, molecular weight, stereochemistry, topology or morphology),
2. The isotherms are only shifted horizontally therefore describing a single relaxation mechanism, and
3. The master curve and shift factor plots are smooth, with no discontinuities, and exhibit a reasonable shape.

1.4.2.1. Modulus Trends

Tachino *et al.*¹⁸ has determined that the extent of ionic character in a polymer directly influences the dynamic mechanical properties of the ionomer. In the study conducted by Tachino *et al.*, the dynamic mechanical properties of EMAA (with 5.4 mol% methacrylic acid units) copolymers and EMAA- Na^+ ionomers were determined as a function of temperature. The dynamic loss modulus is plotted in Figure 1.8.

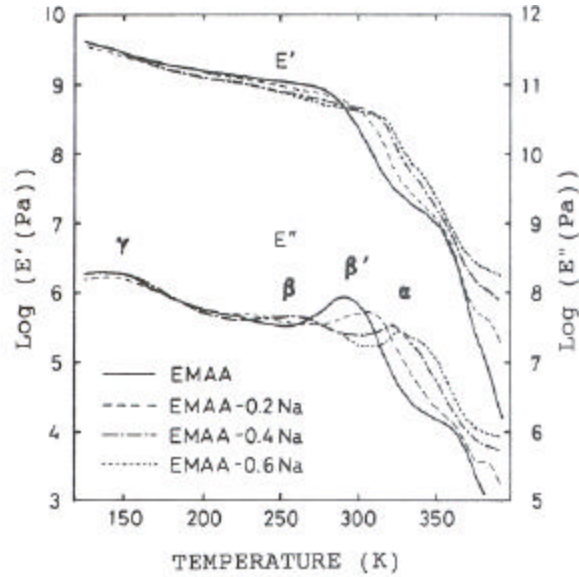


Figure 1.8. Temperature dependence of dynamic storage modulus (E') and loss modulus (E'') at 10 Hz for sodium salts of EMAA ionomers¹⁸.

γ & β' relaxations – small scale molecular motion of short segmental chains in the amorphous regions

β relaxations – motion of the branched amorphous polyethylene chains that contain few un-associated ionic groups

α relaxations – glass-rubber transition of the ionic clusters

The EMAA copolymer showed β' and γ relaxations. The β' relaxation corresponds to micro-Brownian segmental motions in the amorphous regions and the γ relaxation corresponds to local molecular motion of short segmental chains in the amorphous regions. EMAA ionomers neutralized to varying degrees with sodium ions displayed new relaxations that described chain motions specific to ionomers. Instead of exhibiting a β' relaxation, α and β relaxations were observed as presented in Figure 1.8. The α peak corresponds to the glass-rubber transition of the ionic clusters and the β peak corresponds to motion of the branched amorphous polyethylene chains that contain few un-associated ionic groups. An α' relaxation, which superimposed on the α peak, was observed for EMAA-0.60Na ionomers. The α' relaxation is frequency independent and was determined to be a first-order transition corresponding to the order-disorder transition.

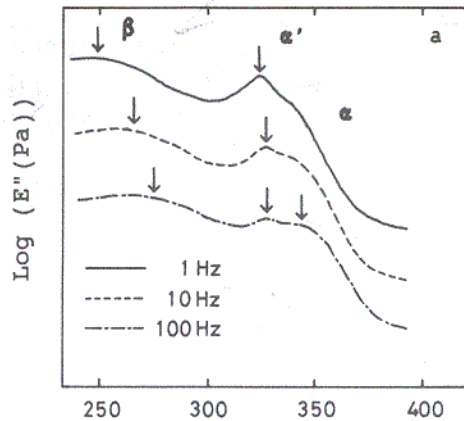


Figure 1.9. Temperature dependence of the dynamic loss modulus (E'') at 1, 10, 100 Hz frequencies for EMAA-0.6Na¹⁸.

β relaxations – motion of the branched amorphous polyethylene chains that contain few un-associated ionic groups

α relaxations – glass-rubber transition of the ionic clusters

α' relaxations – order-disorder transition

In another study by Hirasawa *et al.*¹⁵, the change in stiffness (modulus) of EMAA – zinc neutralized ionomers was investigated with aging time at room temperature. The authors found that stiffness increased with aging time of the EMAA samples, and the extent of the increase in stiffness was dependent on the type and concentration of the cation. The difference in stiffness was correlated with the increase in the ΔH of the order-disorder transition noted in the DSC thermographs. This comparison indicated that stiffness is related to the extent of ionic cluster formation.

Modulus data can also be collected for materials in the terminal zone (melt) using a rheometer. This instrument compliments the DMA in that the data sets from each instrument should overlay. The rheometer can also be used to analyze additional properties of ionomers like viscosity.

1.4.3. Rheometer Background

A rheometer is an instrument used to investigate flow deformation properties of a material via dynamic or steady shear measurements. These measurements are commonly made in parallel plate or cone and plate fixtures. Dynamic oscillation in the rheometer is similar to

performing oscillation in the DMA except terminal relaxations are measured by the rheometer. Shear stresses are applied by sinusoidal oscillation and a phase angle is measured as a function of time and temperature. The ratio of the stress amplitude to strain as a function of time and temperature determine the shear modulus (G). The shear storage modulus (G') represents the elastic behavior and the shear loss modulus (G'') represents the viscous behavior.

Steady shear measurements are unique to the rheometer and are used to measure the flow properties of a material, such as viscosity. When measuring viscosity, a stress is applied to the sample and the rate of strain is measured. Commonly, materials exhibit either Newtonian or non-Newtonian flow behavior. Newtonian behavior occurs when the stress is proportional to the rate of strain. Non-Newtonian behavior occurs when the stress is not proportional to the rate of strain and it is known as shear-thinning (pseudoplasticity). Below is a diagram to illustrate these behaviors (Figure 1.10).

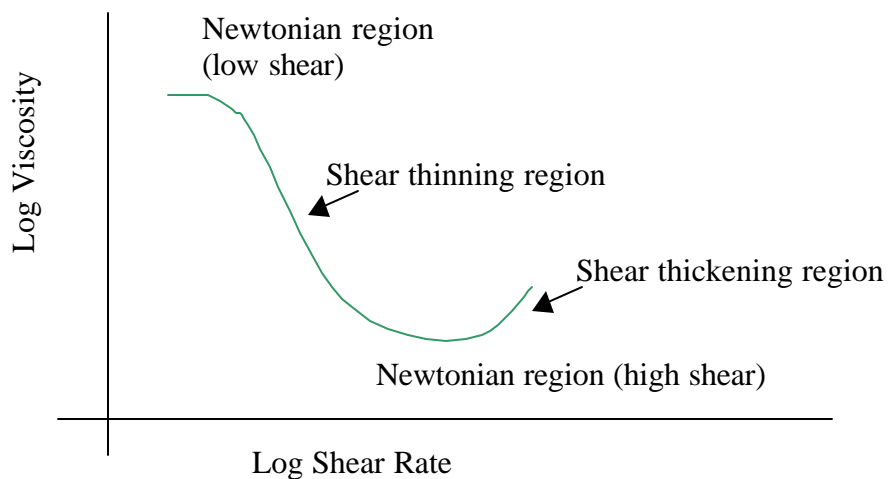


Figure 1.10. Diagram showing the regions of flow behavior, both Newtonian and non-Newtonian¹⁹

1.4.3.1. Viscosity

Vanhoorne *et al.*²⁰ theorized that in the melt, ionomers flow because of a mechanism known as “ion-hopping”. Small angle X-ray scattering experiments have shown that ionic aggregates do not dissociate at temperatures above the order-disorder transition but instead the ionic groups hop between aggregates. Each ionic group has a characteristic lifetime, τ , describing the duration of an ionic group within an individual aggregate. Vanhoorne *et al.* has modeled the

mechanism of ion-hopping and it is illustrated in Figure 1.11. The diffusion (“hopping”) of ionic groups among aggregates permits relaxation of stresses within the segment of polymer chain attached to the ionic group. Due to this relaxation mechanism, macromolecules can diffuse without involving the simultaneous ion-hopping of all the ionic associations along the chain, and the likelihood of this occurring decreases with increasing ionic character. Since the ionic associations act as physical (temporary) crosslinks, there is a net decrease in the diffusion coefficient of the chains resulting in an increase in viscosity.

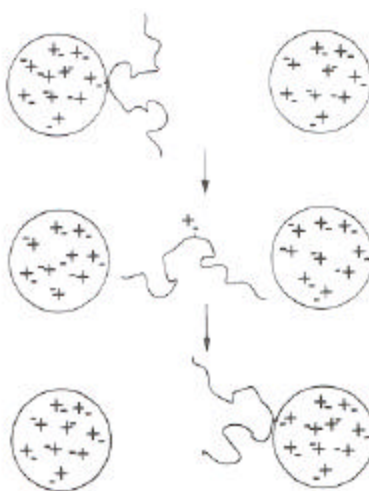


Figure 1.11. Schematic illustrating the “ion hopping” relaxation mechanism in ionomers. The circles represent the ionic aggregates containing the ionic groups, indicated by the positive and negative signs. The area between the aggregates represents the polymer matrix. The curved lines represent a segment of a polymer chain containing a single ionic group. The schematic shows the suggested mechanism of ionic groups moving between aggregates²⁰.

Vanhoorne *et al.* investigated zinc and sodium EMAA ionomers because their terminal relaxation time is short enough to allow for the measurement of melt processes. The ionomers demonstrated Newtonian flow behavior at very low shear rates and therefore true zero-shear viscosities (η_o) were determined. The magnitude of η_o was dependent on the concentration and type of cation in the ionomer, while the recoverable compliance was independent of these factors. The ionomers showed large-scale changes in viscosity compared to their acid copolymer

counter part. During flow, the ionic associations did not tolerate stress and as a result exhibited shorter τ_s than the terminal relaxation time of the polymer chain.

Both the information from the literature using the DSC and DMA will be useful references when characterizing the thermoplastic ionomers in this study.

1.5. Thermoplastic Ionomers

The first thermoplastic carboxylate ionomer was synthesized by DuPont via neutralization of the random copolymers, poly(ethylene-co-methacrylic acid) and poly(ethylene-co-acrylic acid), with alkali metals or zinc hydroxides. This partially or fully neutralized random copolymer was known as Surlyn[®].

Commercially, the acid copolymer is synthesized using free radical chemistry under high pressure conditions.^{4,21} This mechanism of synthesis is similar to that of low-density polyethylene. After the acid copolymer is synthesized, it is dissolved in solution, using tetrahydrofuran for example, and then a basic solution is added. Once all the solvents have been removed, the neutralized copolymer – ionomer - is the final product. The neutralization step can also be achieved in the melt where in a two-roll mill or in an extruder the acid copolymer is fluxed with an aqueous base solution. The water is then removed to produce the ionomer. The extent of neutralization can be determined using infrared spectroscopy and titration of the acid groups.

1.5.1. Nucrel[®] 925

Nucrel[®] 925 is a poly(ethylene-co-methacrylic acid) random copolymer (Figure 1.12), with 5.4 mol % methacrylic acid, synthesized by DuPont. Nucrel[®] 925 is known for its excellent toughness and its low temperature impact properties. It is very lightweight, has high tensile strength, and is very flexible. Nucrel[®] 925 is used for applications in footwear, powder coating, wire and cable, and metal coating.

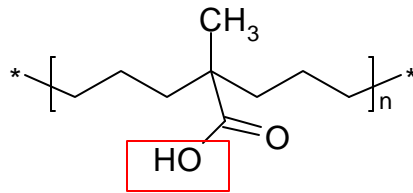


Figure 1.12. EMAA polymer with the acid group (outlined in red)

1.5.2. Surlyn[®]

Surlyn[®] is an ionomer synthesized by DuPont. Surlyn[®] is the random copolymer poly(ethylene-co-methacrylic acid), with 5.4 mol % methacrylic acid (MA), which has been neutralized with a cation (Figure 1.13). Surlyn[®] 8940 has 30% of the 5.4 mol % MA groups neutralized with sodium and Surlyn[®] 8920 has 60% of the 5.4 mol % MA groups neutralized with sodium. Both have excellent clarity, stiffness, and chemical resistance.

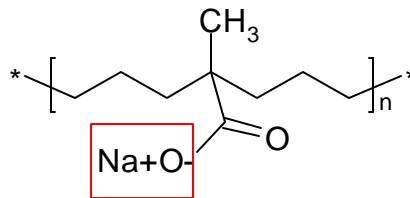


Figure 1.13. EMAA – neutralized with sodium (outlined in red)

Surlyn[®] 8940 is known for its cut resistance and toughness and is used, for example, in ski boots and ice skate shells. Surlyn[®] 8920 is lightweight, has good flex response at low temperature, great toughness, and high impact resistance. It is used in applications such as ski laminating films.

1.5.3. React-A-Seal[®]

React-A-Seal[®] is an ionomer based on Surlyn[®] 8940 and is made by Reactive Target Systems, Inc. React-A-Seal[®] is marketed for its ability to self-heal upon high-speed impact. It has high impact resistance and toughness. It is used in range targets for shooting.

1.6. References

1. Rees, R. W.; Vaughan, D.J. *Polym. Prepr. Am. Chem. Soc. Div. Polym. Chem.* **1965**, *6*, 287-295.
2. Eisenberg, A.; Rinaudo, M. *Polymer Bull.* **1990**, *24*, 671.
3. Eisenberg, A.; Kim, J-S. *Introduction to Ionomers*. John Wiley & Sons, Inc. New York, 1998.
4. Jerome, R.; Mazurek, M. In *Ionomers: Synthesis, Structure, Properties, and Applications*; Tant, M.R., Mauritz, K.A., Wilkes, G.L., Eds.; Chapman and Hall: New York, 1997.
5. Li, C.; Register, R.A.; Cooper, S.L. *Polymer* **1989**, *30*, 1227-1233.
6. Wilson, F.C.; Longworth, R.; Vaughan, D.J. *Polym. Prepr. Am. Chem. Soc., Div. Polym. Chem.*, **1968**, *9*, 505-514.
7. Longworth, R.; Vaughan, D.J. *Nature*, **1968**, *218*, 85-87.
8. Eisenberg, A. *Macromolecules* **1970**, *3*, 147-154.
9. Eisenberg, A.; Hird, B.; Moore, R.B. *Macromolecules* **1990**, *23*, 4098-4107.
10. Marx, C.L.; Caulfield, D.F.; Cooper, S.L. *Macromolecules* **1973**, *6*, 344-353.
11. Yarusso, D.J.; Cooper, S.L. *Macromolecules* **1983**, *16*, 1871-1880.
12. MacKnight, W.J.; Taggart, W.P.; Stein, R.S. *J. Polym. Sci. Symp.* **1974**, *45*, 113-128.
13. Roche, E.J.; Stein, R.S.; Russell, T.P.; MacKnight, W.J. *J. Polym. Sci. Polym. Phys. Ed.* **1980**, *18*, 1497-1512
14. Tadano, K.; Hirasawa, E.; Yamamoto, H.; Yano, S. *Macromolecules*, **1989**, *22*, 226-233.
15. Hirasawa, E.; Yamamoto, H.; Tadano, K.; Yano, S. *Macromolecules*, **1989**, *22*, 2776-2780.
16. Kutsumizu, S.; Tadano, K., Matsuda, Y.; Goto, M.; Tachino, H.; Hara, H.; Hirasawa, E.; Tagawa, H.; Muroga, Y.; Yano, S. *Macromolecules*, **2000**, *33*, 9044-9053.
17. Hatakeyama, T.; Quinn, F.X.; *Thermal Analysis – Fundamentals & Applications to Polymer Science*. John Wiley & Sons: New York, 1994.

18. Tachino, K.; Hara, H.; Hirasawa, E.; Kutsumizu, S.; Tadano, K.; Yano, S. *Macromolecules*, **1993**, *26*, 752-757.
19. Rheology Advantage Instrument Control AR, Product Version V3.0.0; Copyright ©TA Instruments Ltd 1994-2001.
20. Vanhoorne, P.; Register, R. A. *Macromolecules*, **1996**, *29*, 598-604.
21. Longworth, R. In *Developments in Ionic Polymers – I*; Wilson, A.D.; Prosser, H.J., Eds.; Applied Science Publishers: New York, 1983.

2. Experimental

2.1. Materials

The four samples to be characterized in all the following experiments, unless otherwise specified, are Nucrel[®] 925 (EMAA), Surlyn[®] 8940 (EMAA-0.30Na), Surlyn[®] 8920 (EMAA-0.60Na), and React-A-Seal[®] (based on EMMAA-0.30Na). These ionomers will be stored in a desiccator.

2.2. XPS

A XPS spectrum was generated for a bulk sample of React-A-Seal[®] using a Perkin-Elmer Model 5400 XPS spectrometer with a Mg X-ray source (1253.6eV) running at 300W. The pass energy for the wide scan was 44.75eV and for the narrow scan was 17.09eV. The electron take off angle was 45-degrees. A wide scan was run first and then a narrow scan to focus on particular regions of interest. Only one React-A-Seal spectrum was generated.

2.3. TGA

A TA Instruments Hi- Res TGA 2950 was used to investigate degradation properties and moisture content. A temperature ramp was run from room temperature to 600°C at 2.5°C/minute in air. Sample sizes were between 5 and 10 mg.

2.4. DSC

A TA Instruments DSC 2920 equipped with a RCS cooling system was used to study thermal transitions in the four EMMAA samples. A first heat was performed at a temperature ramp from 30°C to 150°C at 5°C/min. The first cooling was performed at a temperature ramp from 150°C to 30°C at 10°C/min. Immediately after a second heat and cooling was performed under the same conditions. The sample size was between 7 and 10mg.

The same DSC was used to investigate the effect of physical aging. The following method was used.

1. The un-aged sample was removed from the desiccator and placed directly into the DSC.
2. In the first heating cycle the temperature was ramped from 30°C to 150°C at 5°C/minute and then cooled to 30°C at 10°C/minute.
3. Immediately the sample was heated to the first aging temperature and held at that temperature for the first aging time.
4. After the elapsed time, the second heating and cooling cycle were performed at the same temperature ramp and heating rate as the first heating cycle.
5. Steps three and four were repeated for each of the aging times (30, 60, 90, and 120 minutes) at each of the aging temperatures (30, 40, 50, 60, 70, 80, and 90°C).

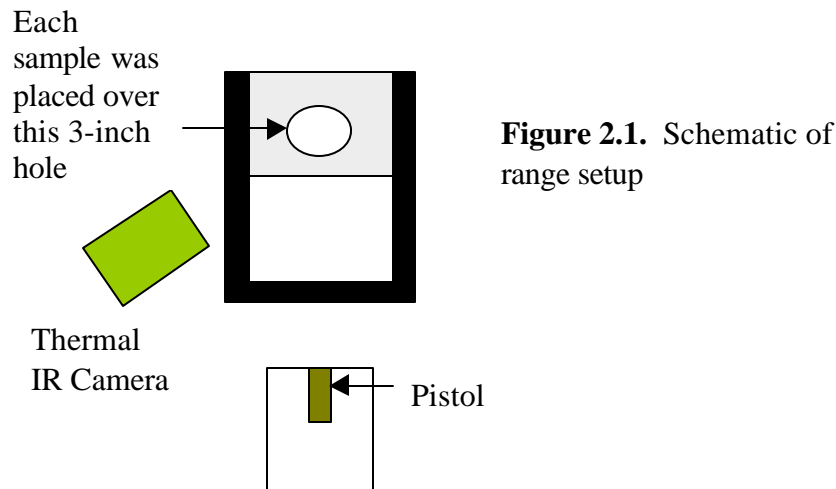
All of the DSC experiments were performed in nitrogen.

2.5. Compression Molding

The React-A-Seal[®] was received in 1/4" sheets. The Nucrel[®] and both Surlyn[®] 8920 and 8940 were received in pellet form. The React-A-Seal[®] was compression molded in the hot press at 115°C with 3000 lbs of pressure for 2 minutes between Kapton[®]. The Nucrel[®] 925 and both Surlyn[®] 8920 and 8940 were compression molded in a hot press at 150°C between Kapton[®] for one minute. While at that same temperature, 7500 lbs of pressure was applied for 30 seconds and then all heat and pressure were removed. All four samples were air cooled at room temperature (~25 to 30°C).

2.6. Pistol Range High-Speed Impact Studies

The high-speed impact studies were used to probe the healing process of the ionomers with the expectation of gaining insight on the healing mechanism. The set up on the range is schematically shown in Figure 2.1. The sample was placed 12 feet from the muzzle of the pistol. The first chronometer, in front of the sample, was 10 feet from the muzzle of the pistol and the second chronometer, behind the sample, was 13 feet from the muzzle. The thermal IR camera was placed to the side of the sample.



A Glock Model 19, 9-mm Parabellum pistol was used to fire the ammunition. The original ammunition used was a Winchester 9-mm Luger 115 Grain Full Metal Jacket bullet (Figure 2.2a) and the standard muzzle velocity was calibrated to 1190 ft/s. These are moderate size bullets that are a versatile standard. The ammunition is easily reloaded to afford different velocities. Nucrel[®] 925, Surlyn[®] 8940, Surlyn[®] 8920, and React-A-Seal[®] were shot at ambient temperature (~28°C) with standard 9-mm bullets at various velocities ranging from ~1200 ft/s to ~300 ft/s. In addition, blunt ended cylindrical bullets loaded to 115 grains were tested at ambient temperature (~28°C) with a velocity of 1100ft/s. The blunt ended cylindrical bullets are 9-mm bullets loaded backwards (Figure 2.2b). By varying the velocities and shape of the bullets, it was expected that a change in the healing phenomenon would occur.



Figure 2.2. (a) Shows a standard 9mm bullet, (b) shows a blunt ended cylindrical bullet

2.7. DMA

A TA Instruments DMA 2980 was used to measure both dynamic loss modulus and creep/creep recovery.

For the dynamic modulus data, the dual cantilever clamp and a bar shaped sample were used. The EMAA samples were tested at a temperature ramp from -130°C to 90°C at 3°C increments. An amplitude of 25 μm was arbitrarily chosen as it did not exceed the load limit for the instrument. At each temperature three frequencies were swept, 1, 10, and 100 Hz. This measurement was made 9 days after the four samples had been melt processed.

For the creep/creep recovery experiments, the compression clamp and a cylindrical sample (diameter 3/16") were used. The diameter of the probe was 2.82 mm and this diameter was used in the area calculation rather than the diameter of the sample. A static force, 0.01 N, was maintained throughout the entire experiment. The stress applied during creep was 1.5 MPa and creep was measured for 60-minutes. The stress applied during creep recovery was 0 Pa and creep recovery was measured for 60-minutes.

2.8. Rheometer

The TA Instruments Advanced Rheometer 1000 was used to make the viscosity measurements. The parallel plate geometry was used and the plates had a diameter of 25 mm. For all the experiments, the working gap was 1.8 - 1.9-mm. Viscosity was measured at 90, 110, 130, and 150°C. Shear stresses between 0.03259 and 32590 Pa were measured for 20 minutes with 150 sampling points.

3. Results and Discussion

Physical, Thermal, and Mechanical Characterization

3.1. XPS of React-A-Seal[®]

The React-A-Seal[®] has an opaque appearance compared to the Surlyn[®] 8940. This was the first indication that the React-A-Seal[®] contained some unknown additives. To determine whether this was true, XPS analysis was performed on the React-A-Seal[®].

Surlyn[®] 8940 is the primary component of React-A-Seal[®] and it is composed of carbon, oxygen, and sodium. From the XPS spectra of the bulk React-A-Seal[®], it was established that the ionomer also contained silicon and nitrogen. The atomic concentrations were determined from the area of the elemental peaks. Table 3.1 contains the pertinent information from the analysis.

Table 3.1
Data from React-A-Seal[®] XPS spectra

Element	Atomic Concentration (%)
C (1s)	87.7
O (1s)	8.1
N (1s)	1.3
Si (2p)	2.0
Na (1s)	0.9

Notice that carbon and oxygen make up approximately 96% of the atomic concentration and ~1% is sodium. It could be initially concluded that the unknown additive is composed of the 2% silicon and 1.3% nitrogen.

The XPS data can be further interpreted with the structure of methacrylic acid (Figure 3.1).

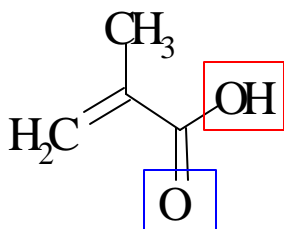
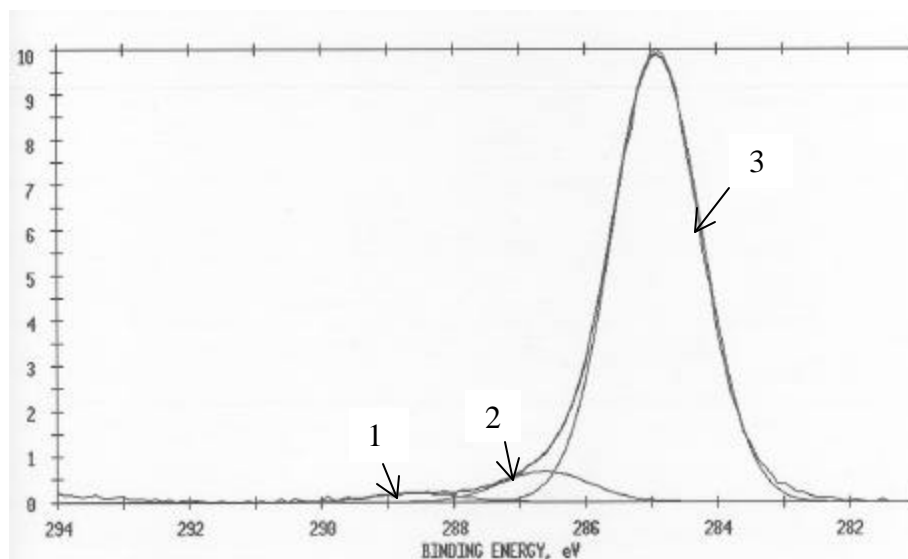


Figure 3.1. Structure of methacrylic acid – hydroxyl group outlined in red, the carboxyl group outlined in blue

Methacrylic acid has two oxygen atoms, one in the carboxyl group and one in the hydroxyl group; consequently, the detected oxygen should be split between the hydroxyl and the carboxyl groups. The oxygen in the hydroxyl group is the only oxygen neutralized with sodium and according to DuPont, 30% of the hydroxyl groups are neutralized. So, sodium should have an atomic concentration of 1.35%; however, the detected atomic concentration of sodium is 0.9%. Thus, it can be speculated that not all of the oxygen detected is coming from the methacrylic acid groups; a portion is possibly coming from the silicon/nitrogen additive.

Figure 3.2 shows the curve-fit for the C 1s and O 1s peaks in a narrow scan spectra. Table 3.2 shows the peak assignments for the C 1s and O 1s curve-fit peaks. The curve fits and peak assignments were performed using reference binding energies from Beamsom and Briggs¹⁰. As expected, ester bonds, hydrocarbon bonds, hydroxide bonds, and carbon-oxygen bonds were curve fit in the peak analysis.

a)



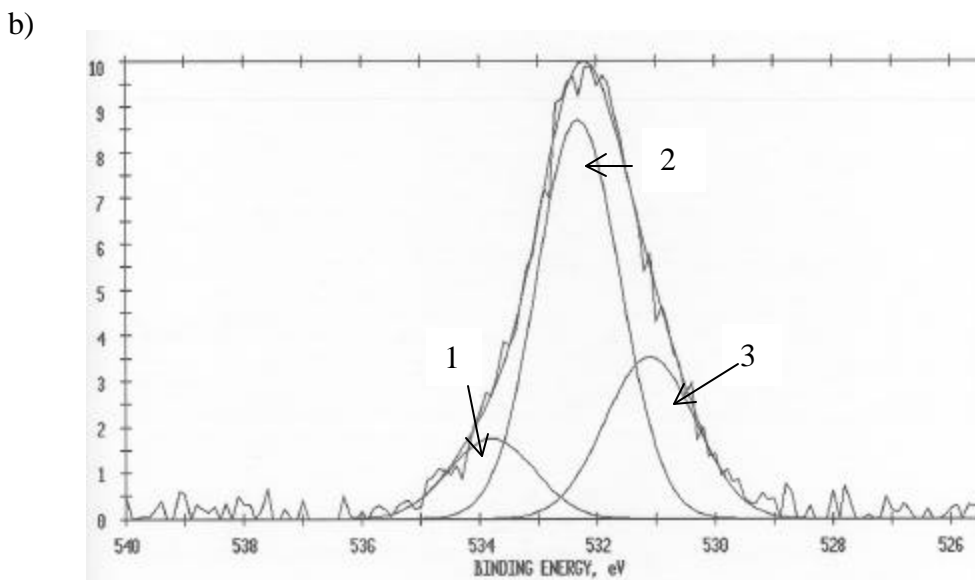


Figure 3.2. Curve-fit for the C 1s and O 1s peaks from React-A-Seal[®] XPS narrow scan

Table 3.2

React-A-Seal[®] peak assignments for C 1s and O 1s from the curve-fit narrow

	Peak 1	Peak 2	Peak 3
(a) Carbon 1s	Ester C=O	C—O	Hydrocarbon C—H
(b) Oxygen 1s	Hydroxide O—H	O—C Siloxane Si—O	Ester C=O

The Si 2p peak was detected at 102 eV. Given this binding energy, the Si 2p peak is likely due to chemical bonding of the silicon to form siloxane or silicate linkages. If the peak were at 99 eV, then the peak would likely be a result of elemental silicon in the form of a filler. Si—O bonding was detected from the O 1s peak. Si—C bonds were not detected in the C 1s peak due to either the overwhelming concentration of carbon compared to silicon, or because there were no Si—C bonds formed. A Si—C linkage could be expected because the silicon requires four bonds, thus could bond to oxygen only or could bond to both oxygen and carbon.

From the XPS data it is difficult to determine how silicon was chemically bonded in the React-A-Seal[®]. Possibly, the detected nitrogen is a byproduct of an unknown chemical reaction, whether as a catalyst or a component of the type of silicon used.

With the compositional information about React-A-Seal[®], and recalling the known composition of Nucrel[®] 925 (EMMA), Surlyn[®] 8940 (EMMA-0.30 Na), and Surlyn[®] 8920 (EMMA-0.60 Na), more meaningful information can now be collected about the degradation properties of these ionomers.

3.2. TGA

Figure 3.3 shows a graph of weight percent as a function of temperature for Nucrel[®] 925, Surlyn[®] 8940, React-A-Seal[®], and Surlyn[®] 8920. Table 3.3 shows the temperatures for each sample corresponding to 2, 10, and 95% weight loss in air.

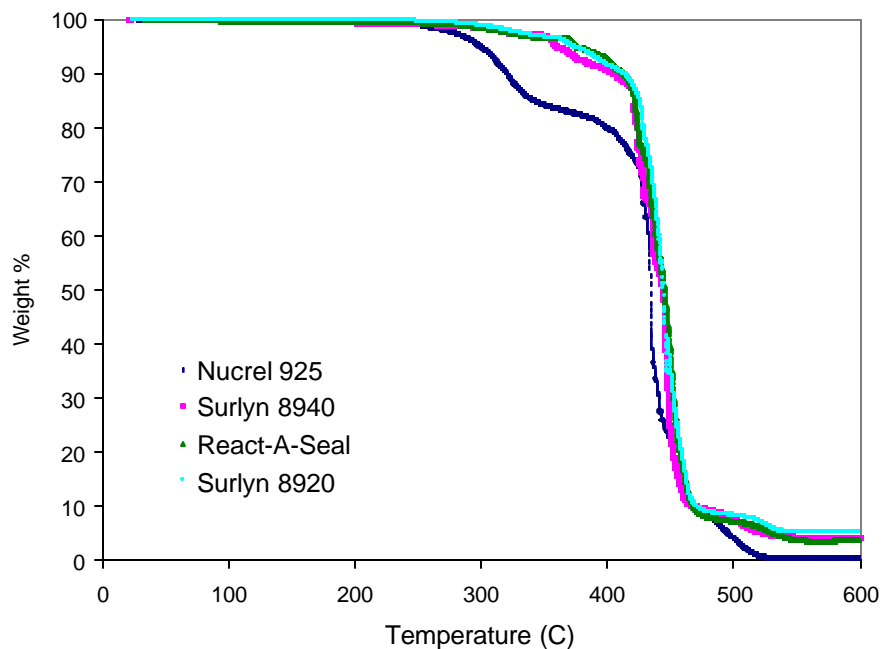


Table 3.3

Degradation temperatures for each sample at 2, 10, and 95% weight loss

	Wt % Na ⁺	Weight Loss		
		2 %	10 %	90 %
Nucrel [®] 925	0%	274°C	320°C	469°C
Surlyn [®] 8940	30%	312°C	404°C	469°C
React-A-Seal [®]	30%	313°C	412°C	468°C
Surlyn [®] 8920	60%	322°C	413°C	471°C

With increase in ionic content, the temperature for degradation at 90% weight loss did not significantly change. Differences in the curves are due to changes in the thermal stability of the EMAA samples.

Surlyn[®] 8940, React-A-Seal[®], and Surlyn[®] 8920 were more thermally stable than Nucrel[®] 925. At the conclusion of the TGA experiments a charred residue from Surlyn[®] 8940, React-A-Seal[®], and Surlyn[®] 8920 was noticed in the TGA pans. According to McNeill *et al.*⁹, the residue was possibly sodium carbonate although the precise pathway for degradation of ethylene ionomers is uncertain. XPS analysis was performed on the Surlyn[®] 8940, React-A-Seal[®], and Surlyn[®] 8920 residues and the composition data are presented in Table 3.4.

Table 3.4

Data from XPS spectra of Surlyn[®] 8940, React-A-Seal[®] and Surlyn[®] 8920 TGA pan residue

Element	Atomic Concentration
C 1s	22.1 %
O 1s	52.9%
Na 1s	25.0%

The detection of carbon, oxygen, and sodium support the possibility that the TGA residue from the EMAA ionomers is sodium carbonate. The carbon and oxygen peaks could not be resolved due to interference from the sodium peaks, so functionality could not be determined.

The degradation pathway for Nucrel[®] 925 is well understood⁸. Nucrel[®] 925 exhibited two degradation regions, (1) 260°C to 345°C and (2) 345°C to 406°C. According to Inai *et al.*⁸, the first degradation region (1) corresponds to the conversion of EMAA into linear-type anhydrides. The second degradation region(2) corresponds to the thermal degradation of the linear-type anhydrides and of the main polymer chains.

Moisture loss could be detected from the TGA degradation curves of Nucrel[®] 925, Surlyn[®] 8940, React-A-Seal[®], and Surlyn[®] 8920 because their decomposition in air is a process that produces water at ~100°C. Less than 0.2 % moisture loss occurred at 100°C for Nucrel[®] 925, Surlyn[®] 8940, React-A-Seal[®] and Surlyn[®] 8920. Studies^{1,2,3} have shown, that water coordinates rather easily with sodium ionomers and affects their physical and mechanical properties. In order to maintain consistency among the samples for the physical and mechanical testing, specimens were stored in a desiccator prior to any further testing.

The degradation characteristics of the Nucrel[®] 925, Surlyn[®] 8940, React-A-Seal[®] and Surlyn[®] 8920 denote the viable temperature range for further thermal analysis using DSC.

3.3. DSC

Typical DSC curves, as observed in literature^{1,8}, are presented in Figure 3.4 for Nucrel[®] 925, Surlyn[®] 8940, React-A-Seal[®], and Surlyn[®] 8920. Notice that in the first heat (1H), the order-disorder transition (T_i) at ~52°C occurred prior to the crystalline melting peak. In the second heat (2H), the order-disorder transition was depressed, yet the crystalline melting peak occurred at the same temperature. Table 3.5 shows the peak temperature values for the order-disorder transition.

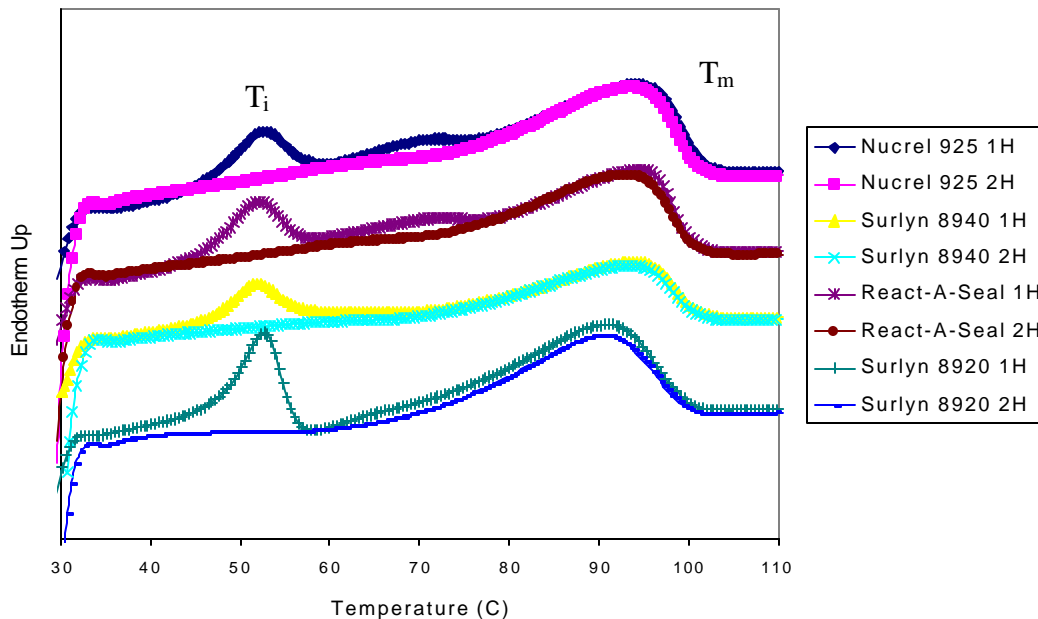


Figure 3.4. First heat (1H) and second heat (2H) for the Nucrel[®] 925, Surlyn[®] 8940, React-A-Seal[®], and Surlyn[®] 8920 from the DSC

Table 3.5
Maximum temperature of order-disorder transition

	Wt % Na ⁺	T _{max} of T _i transition
Nucrel [®] 925	0%	52.5°C
Surlyn [®] 8940	30%	51.9°C
React-A-Seal [®]	30%	52.2°C
Surlyn [®] 8920	60%	52.6°C

As expected, the order-disorder transition was observed for Surlyn[®] 8940, React-A-Seal[®], and Surlyn[®] 8920. This order-disorder transition was at approximately the same temperature for the three EMAA ionomers, ~52°C. Unexpectedly, the Nucrel[®] 925 showed a transition similar to the ionomer samples at ~52°C. Polar attractions between acrylic acid moieties may be related; but the actual origin is unknown. However, the similarity of the peak to

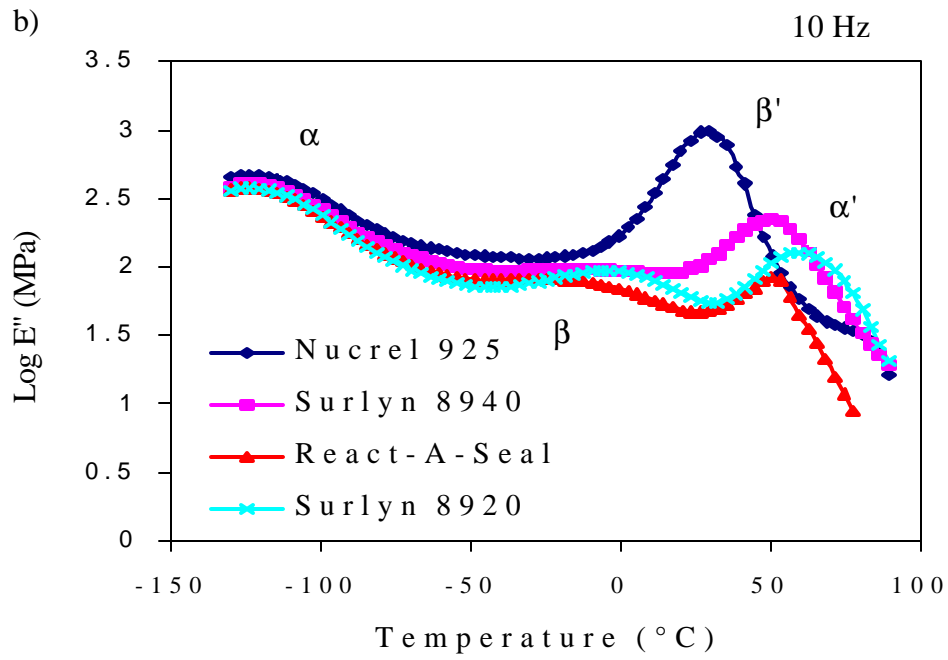
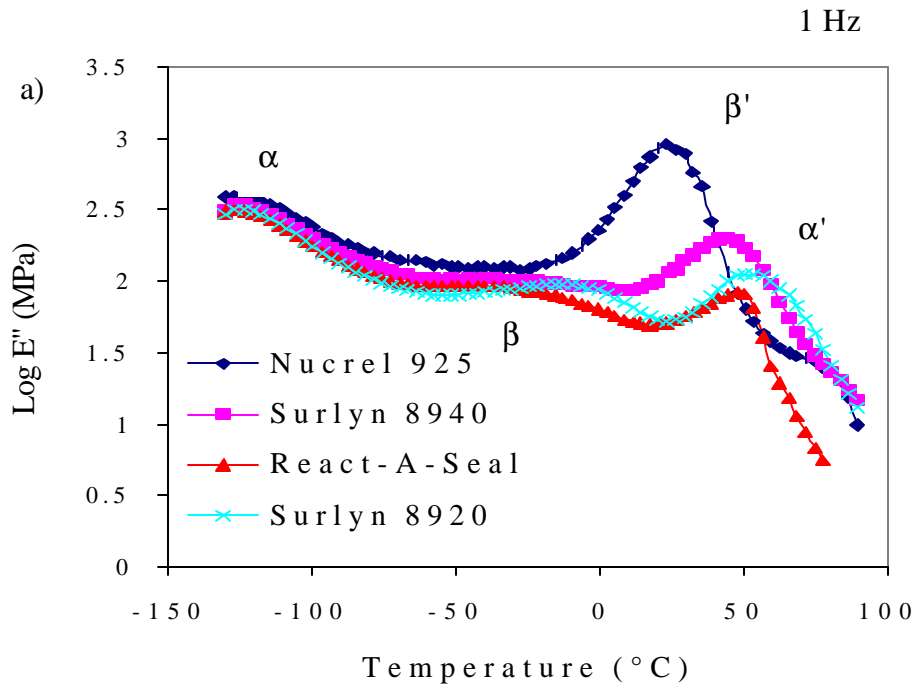
those of the ionomers clearly suggests a similar structural change. Therefore, the observed Nucrel[®] 925 transition is possibly an ordering and disordering of weak carboxyl aggregations.

Hird *et al.*⁴ have suggested three possible mechanisms for the order-disorder transition in ionomers. The first mechanism assumes that the rigidity (modulus) and strength (breaking stress) of the aggregates is conserved at all temperatures. The T_i occurs when the temperature is increased enough to cause motions resembling those of a glass transition. The second mechanism assumes that only the strength of the aggregates is conserved with temperature change. With an increase in temperature, the rigidity decreases and the mobility of the aggregates increases until enough polymer chain motion occurs to bring about a glass transition. The last mechanism assumes that ion-hopping occurs near the glass transition resulting in a decrease in the rigidity and strength of the aggregates. No proof exists for any of the above mechanisms, although Hird and Eisenberg⁵ have found evidence for ion-hopping at T_i for sulfonated styrene ionomers. The results in this present DSC study do not distinguish any one of the above mechanisms.

Recall that ionomers have two phases, a polymer matrix phase, made up of the ethylene and un-reacted MA backbone, and an ionic phase, made up of the neutralized MA groups. Reportedly⁶, it can be difficult to detect both a T_g for the polymer matrix and a T_i for the ionic clusters due to the sensitivity of DSC and the size of the clustered ionic regions. Also, in DSC, a T_g would be difficult to detect because polyethylene copolymers are semi-crystalline. For Nucrel[®] 925, Surlyn[®] 8940, React-A-Seal[®], and Surlyn[®] 8920 DSC only detected a T_i , no T_g , and little was learned about molecular motions of the polymer chains. To learn more about the undetected thermal motions, data were collected from the DMA.

3.4. DMA

Figure 3.5 shows the temperature dependence of the dynamic mechanical properties of Nucrel[®] 925, Surlyn[®] 8940, React-A-Seal[®], and Surlyn[®] 8920 at 1, 10, and 100 Hz nine days after they had been melt pressed.



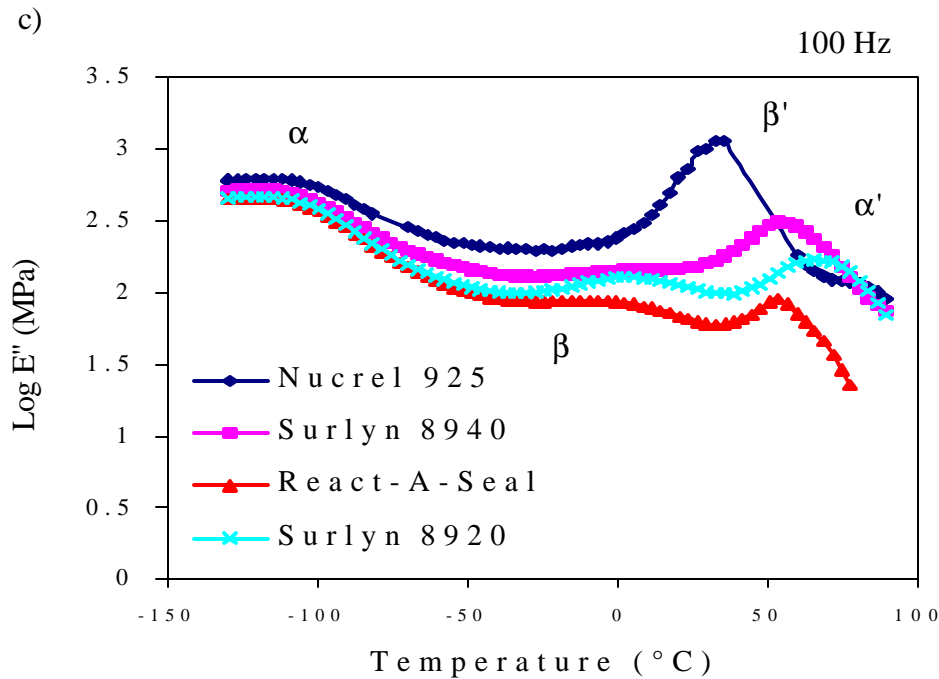


Figure 3.5. Temperature dependence of dynamic loss modulus (E'') at (a) 1 Hz, (b) 10 Hz, and (c) 100 Hz – The α , α' , β , and β' designations are a result of the Arrhenius analysis

An Arrhenius analysis was used to evaluate the activation energies (E_a) of the relaxations given in Figure 3.5. The Arrhenius equation is shown below where ω is frequency.

$$\omega = \omega_0 \exp\left(\frac{-E_a}{RT}\right)$$

$$\ln \omega = \ln \omega_0 - \left(\frac{E_a}{RT}\right)$$

By plotting the natural log of ω versus reciprocal temperature (Kelvin), the slope of the resulting linear line is proportional to the activation energy, which describes the difficulty of activating the motion of the measured relaxation. Figure 3.6 shows an example of an Arrhenius plot for the α relaxation in React-A-Seal[®].

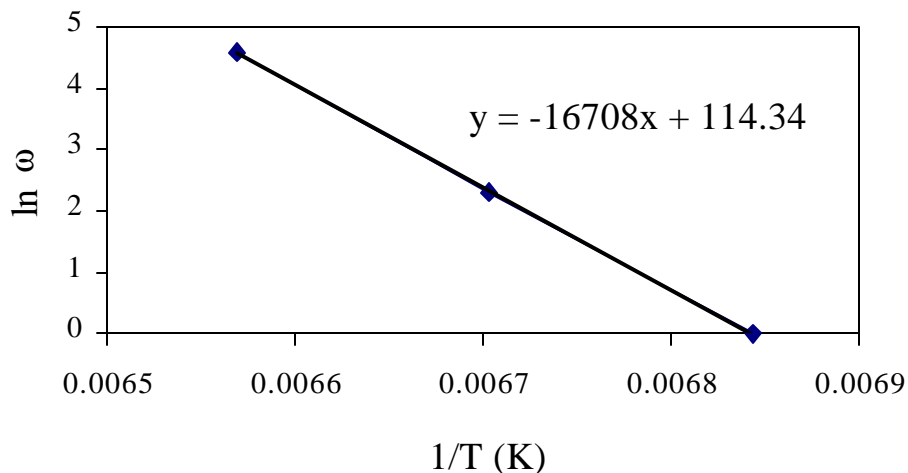


Figure 3.6. An Arrhenius plot for the α relaxation in React-A-Seal[®]. The slope is proportional to activation energy of that relaxation, $E_a = -\text{slope} * \text{gas constant}(R)$

Table 3.6 lists the calculated activation energy of each relaxation and a designation for the relaxations in Nucrel[®] 925, Surlyn[®] 8940, React-A-Seal[®], and Surlyn[®] 8920.

Table 3.6

Activation energies for the relaxations of each sample with peak designations
 α relaxation – glass-rubber transition of the polymer matrix
 β' relaxation – micro-Brownian segmental motion in the amorphous regions
 β relaxation – motion of the branched amorphous polyethylene chains that contained few unassociated ionic groups
 α' relaxation – order-disorder transition of the ionic aggregates

Sample	Activation Energies (kJ/mol) of Relaxations Exhibited in the Dynamic Loss Modulus Data			
	α	β	β'	α'
Nucrel [®] 925	92.9	-	291.4	-
Surlyn [®] 8940	140.2	46.3	-	666.6
React-A-Seal [®]	138.9	70.2	-	663.4
Surlyn [®] 8920	141.8	181.4	-	-

Typically, if the activation energy of a polymer relaxation is greater than 100 kJ/mol, then that relaxation is attributed to a glass-rubber transition (α). If the activation energy is less than 100 kJ/mol then the relaxation is attributed to smaller scale micro-Brownian segmental motion in the amorphous regions, or small side chain or end group motions (β and γ). Tachino *et al.*⁷ measured a γ relaxation at -130°C with an activation energy of ~ 40 kJ/mol. Nucrel[®] 925, Surlyn[®] 8940, React-A-Seal[®], and Surlyn[®] 8920 exhibited a relaxation at $\sim -120^{\circ}\text{C}$. Due to the activation energy of the relaxation in Surlyn[®] 8940, React-A-Seal[®], and Surlyn[®] 8920 (> 100 kJ/mol) and the fact that polyethylene has a T_g of ~ -120 to -130°C , the relaxation ($\sim -120^{\circ}\text{C}$) was assigned to the polymer matrix T_g (α). Nucrel[®] 925 had a smaller activation, 92.9 kJ/mol yet, considering the T_g of polyethylene, the relaxation was attributed to the glass-rubber transition of the polymer matrix.

Tachino *et al.* measured (at 10 Hz) a β' relaxation, corresponding to micro-Brownian segmental motion in the amorphous regions, for peaks at 18°C for the EMAA copolymer and at 32°C for the EMAA- Na^+ ionomers that were neutralized to 20%. The β' activation energy for the EMAA copolymer was 246 kJ/mol. The β' activation energy for the EMAA-0.20Na ionomers was ~ 260 kJ/mol. For EMAA- Na^+ ionomers neutralized to 40% and above, Tachino *et al.* measured (10 Hz), a β relaxation at $\sim -13^{\circ}\text{C}$, corresponding to motion of the branched amorphous polyethylene chains that contained few unassociated ionic groups, and an α' relaxation at $\sim 52^{\circ}\text{C}$ corresponding to the order-disorder transition. The β relaxation had an activation energy of ~ 110 kJ/mol and did shift with frequency. Tachino *et al.* did not report an activation energy for the α' relaxation but observed that it did not shift with frequency. Tachino *et al.* concluded that the observation of α' and β relaxations indicated phase separation of ionic regions from the polyethylene matrix and the formation of ionic clusters⁷.

In the present research, Nucrel[®] 925 showed a β' relaxation which agreed well with the data from Tachino *et al.*⁷ in both its shape and activation energy. Surlyn[®] 8940 and React-A-Seal[®], both neutralized to 30%, did not produce the β' relaxation. Instead Surlyn[®] 8940 and React-A-Seal[®] showed a β relaxation at $\sim -15^{\circ}\text{C}$ that corresponded to a typical polymer β relaxation with respect to the measured activation energy (< 100 kJ/mol). Surlyn[®] 8920 also exhibited the β relaxation, although the activation energy was higher than that measured by

Tachino. It would be expected that Surlyn[®] 8920 would show a β relaxation at a higher temperature and with a higher activation energy than Surlyn[®] 8940 and React-A-Seal[®]. Surlyn[®] 8920 has the greatest extent of aggregation, 60% of the MA groups are neutralized, and no movement of the clustered regions is expected near the temperature of the measured β relaxation. This immobilization of the clustered regions restricts the motion of the adjacent polyethylene regions, more in the Surlyn[®] 8920 than in Surlyn[®] 8940 or in React-A-Seal[®], which are both only 30% neutralized, and thus Surlyn[®] 8920 requires more energy for motion.

Surlyn[®] 8940 and React-A-Seal[®] exhibited an α' relaxation, order-disorder transition of the ionic aggregates, at $\sim 50^\circ\text{C}$ (10 Hz). This relaxation was frequency dependent, with the relaxation shifted to higher temperatures at higher frequencies as expected. However, this result contradicts the frequency independence of the α' relaxation as measured by Tachino *et al.* Surlyn[®] 8920 also yielded an α' relaxation showing frequency dependence but the temperature at which it occurred varied significantly (shown in Table 3.6). This deviation in temperature could be due to the higher ionic concentration in Surlyn[®] 8920 compared to Surlyn[®] 8940 and React-A-Seal[®].

Table 3.7

Comparison of the measured temperatures of the order-disorder transition in the DSC and the temperature of the α' relaxation from the loss modulus curve in Figure 3.5

Sample	DSC T_i	T_{\max} of the α' relaxation at 1,10, and 100 Hz		
		1 Hz	10 Hz	100 Hz
Nucrel [®] 925	52.5°C	-	-	-
Surlyn [®] 8940	51.9°C	47.2	50.2	53.2
React-A-Seal [®]	52.2°C	47.3	50.3	53.3
Surlyn [®] 8920	52.6°C	50.3	59.3	65.3

Two replicate DMA-frequency measurements were performed on Nucrel[®] 925 and activation energies were calculated for the α and β' relaxations observed in the six dynamic loss

curves. The average activation energy of the α relaxation was 92.9 ± 0.063 kJ/mol. The average activation energy of the β' relaxation was 322.1 ± 43.2 kJ/mol. It was assumed that the errors calculated for the activation energies in Nucrel[®] 925 were similar to the expected errors for Surlyn[®] 8940, React-A-Seal[®], and Surlyn[®] 8920.

For more insight on the viscous and elastic behaviors of the Nucrel[®] 925, Surlyn[®] 8940, React-A-Seal[®], and Surlyn[®] 8920, the DMA was used to measure creep and creep recovery in the glassy and rubbery region. The results are presented in the next section.

3.5. References

1. Hirasawa, E.; Yamamoto, Y. *Macromolecules* **1989**, *22*, 2776-2780.
2. Kutsumizu, S.; Tadano, K.; Matsuda, Y.; Goto, M.; Tachino, H.; Hara, H.; Hirasawa, E.; Tagawa, H.; Muroga, Y.; Yano, S. *Macromolecules* **2000**, *33*, 9044, 9053.
3. Tachino, H.; Hara, H.; Hirasawa, E.; Kutsumizu, S.; Yano, S. *J. Applied Polym. Sci.* **1995**, *55*, 121-138.
4. Hird, B.; Eisenberg, A. *Macromolecules* **1992**, *25*, 1203 -1206.
5. Hird, B.; Eisenberg, A. *Macromolecules* **1992**, *25*, 6466 - 6474.
6. Eisenberg, A.; Kim, J-S. *Introduction to Ionomers*. John Wiley & Sons, Inc. New York, 1998.
7. Tachino, H.; Hara, H.; Hirasawa, E.; Kutsumizu, S.; Tadano, K.; Yano, S. *Macromolecules* **1993**, *26*, 752-757.
8. Inai, Y.; Kato, S.; Hirabayashi, T.; Yokata, K. *Polymer Journal* **1995**, *27*, 196-200.
9. McNeill, I.C.; Alston, A. *De Angewandte Makromolekulare Chemie* **1998** *261/262*, 157-172.
10. Beamson, G.; Briggs, D. *High-Resolution XPS of Organic Polymers – The Scienta ESCA 300 Database*. John Wiley & Sons, Inc. New York, 1992.

4. Results and Discussion

Viscoelastic Characterization

4.1. DMA

Creep and creep recovery experiments were performed in the compression geometry (Figure 4.1) to better understand the viscoelastic characteristics exhibited by Nucrel[®] 925 (EMAA), Surlyn[®] 8940 (EMAA-0.30Na), React-A-Seal[®] (based on EMAA-0.30Na), and Surlyn[®] 8920 (EMAA-0.60Na).

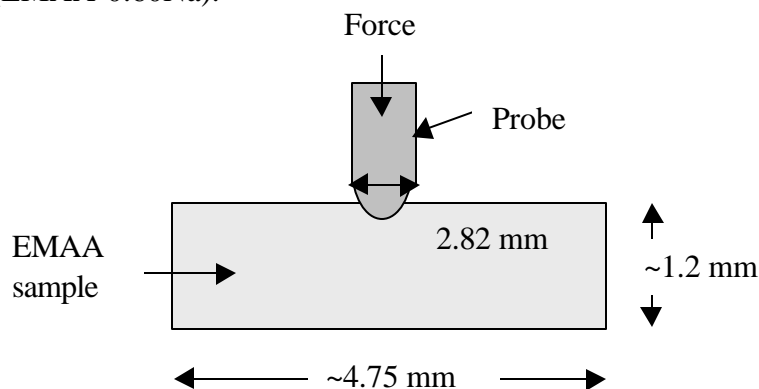


Figure 4.1. Schematic of the compression geometry - the amount of penetration by the probe is dictated by the temperature and stress applied in the experiment

The creep curves describe the displacement response of the ionomers when given a constant stress as in Figure 4.1. Figures 4.2, 4.3, 4.4, and 4.5 show the creep curves as a function of time at varying temperatures for Nucrel[®] 925, Surlyn 8940[®], React-A-Seal[®], and Surlyn 8920[®], respectively. The EMAA samples showed minimal creep at low temperatures and significantly larger creep at higher temperatures.

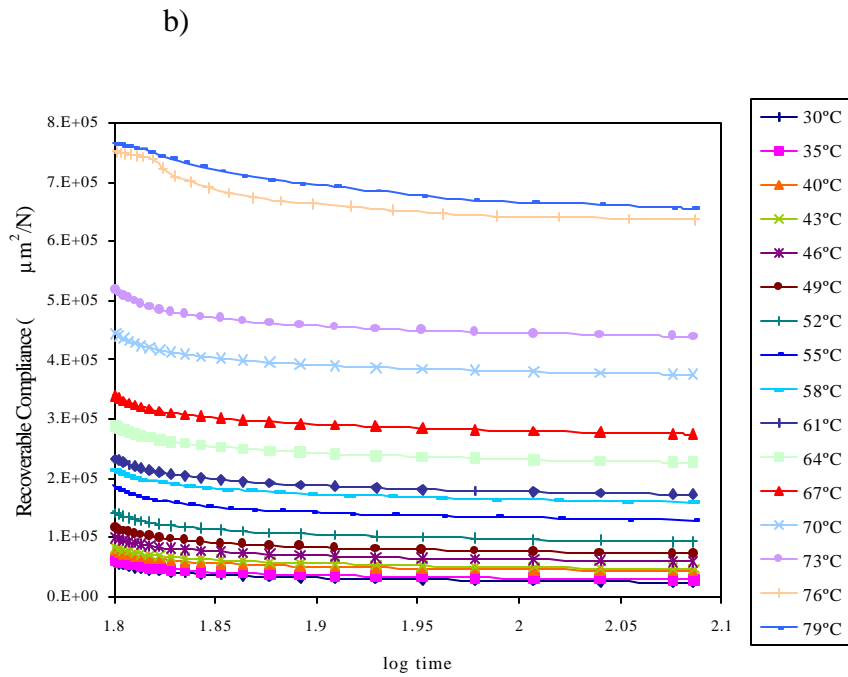
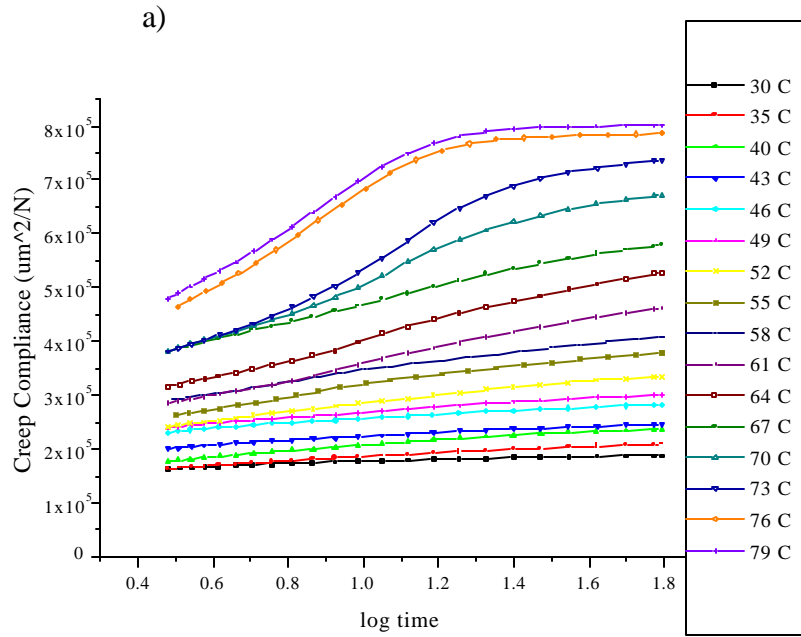


Figure 4.2. (a) Creep isotherms at 1.5 MPa stress and (b) creep recovery isotherms at 0 MPa stress for Nucrel[®] 925 at temperatures between 30°C and 79°C

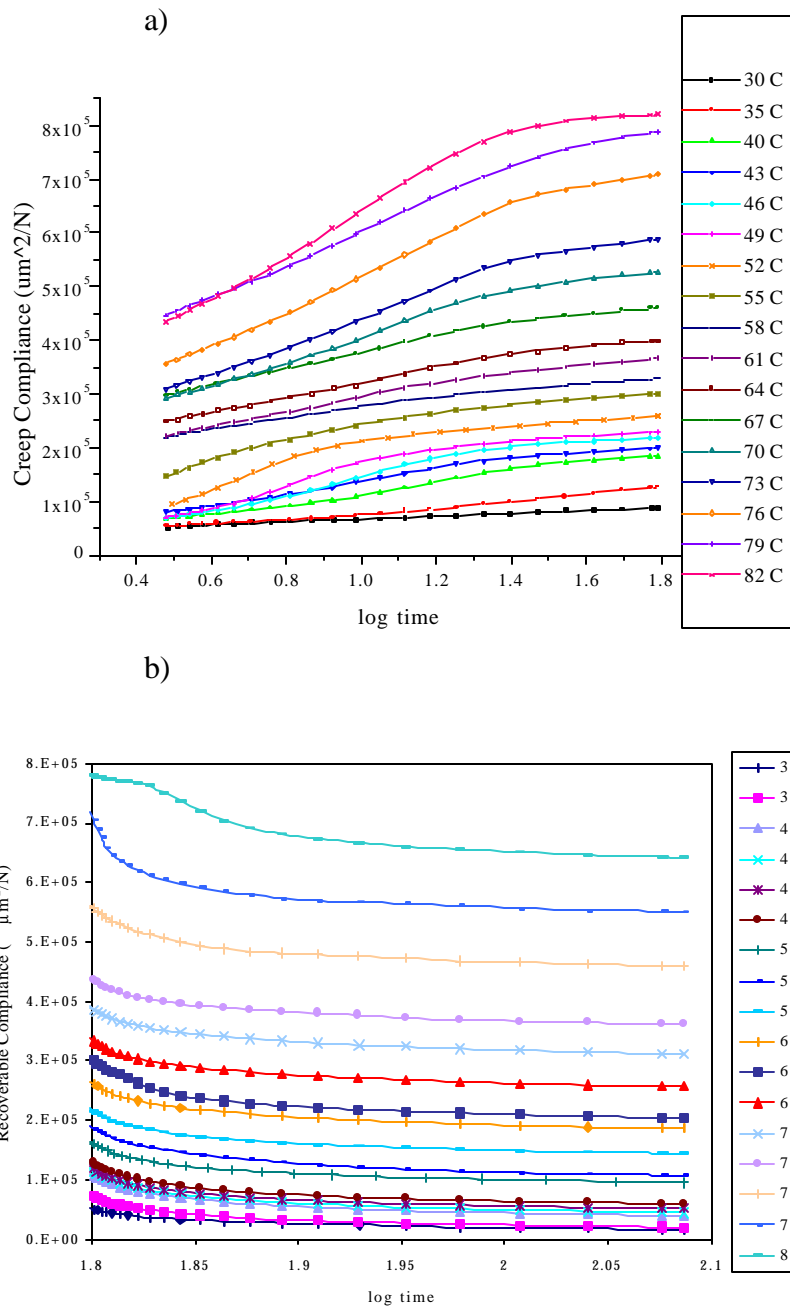


Figure 4.3. (a) Creep isotherms at 1.5 MPa stress and (b) creep recovery isotherms at 0 MPa stress for Surlyn[®] 8940 at temperatures between 30°C and 82°C

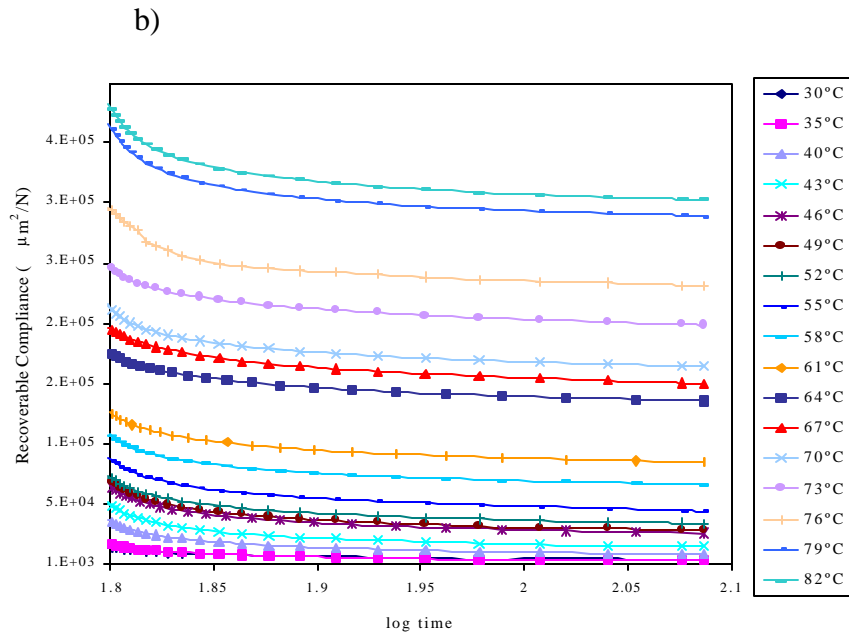
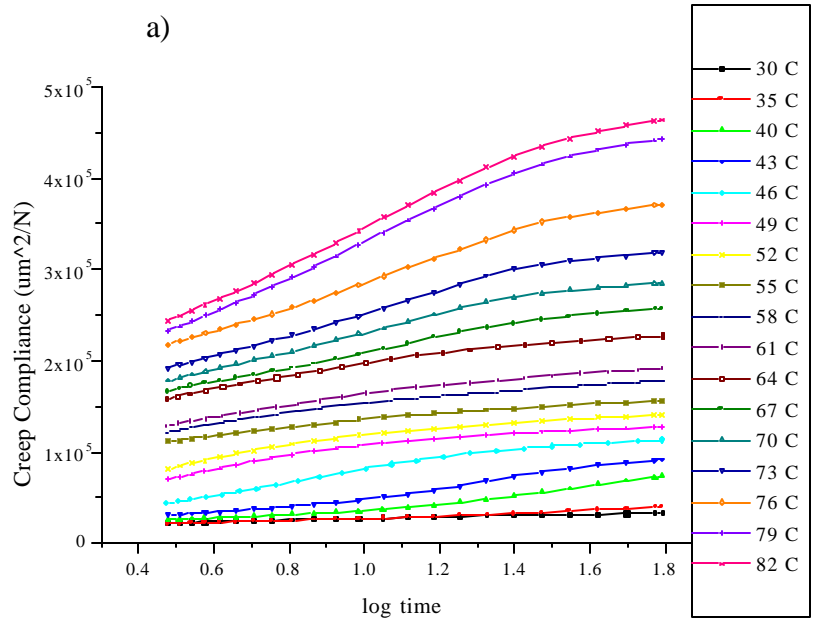


Figure 4.4. (a) Creep isotherms at 1.5 MPa stress and (b) creep recovery isotherms at 0 MPa stress for React-A-Seal[®] at temperatures between 30°C and 82°C

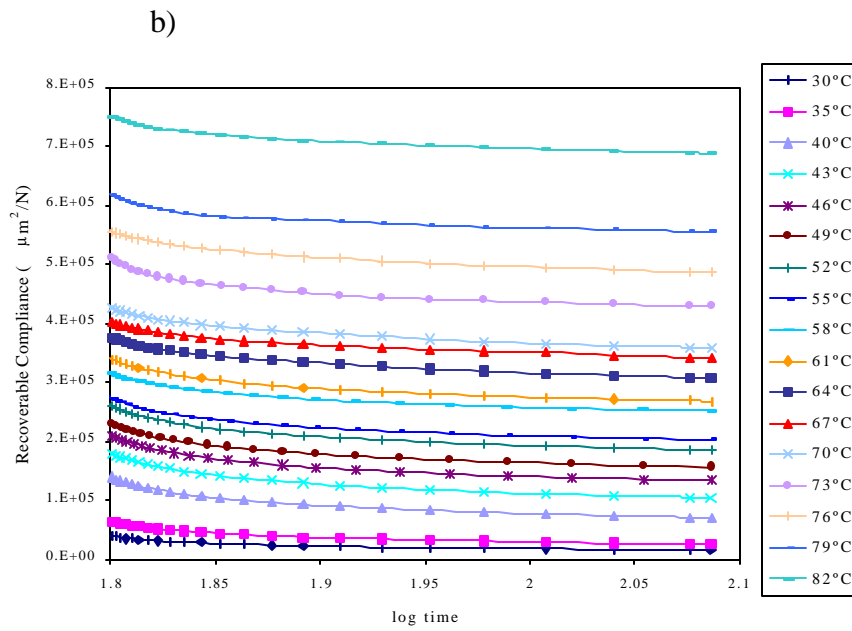
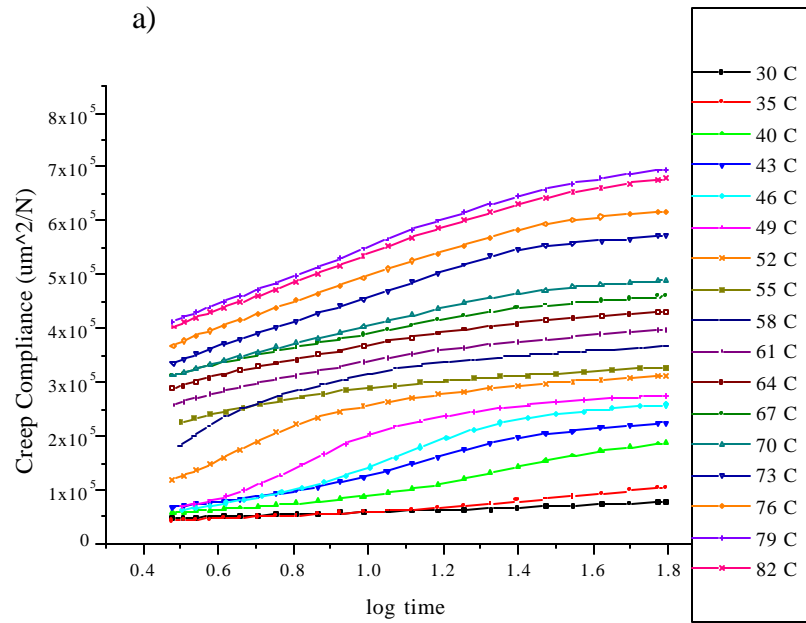


Figure 4.5. (a) Creep isotherms at 1.5 MPa stress and (b) creep recovery isotherms at 0 MPa stress for Surlyn[®] 8920 at temperatures between 30°C and 82°C

Nucrel[®] 925, Surlyn[®] 8940, and Surlyn[®] 8920 displayed approximately the same magnitude of compliance (a measure of softness) at the higher test temperatures. React-A-Seal[®] was expected to have a similar creep response to the Surlyn[®] 8940, considering that React-A-Seal[®] is primarily comprised of Surlyn[®] 8940. However, React-A-Seal[®] had a smaller compliance, about half as large as the Surlyn[®] 8940, at the higher test temperatures. This smaller compliance (increase in stiffness) may be due to the silicon-based additive, detected by XPS, in the React-A-Seal[®]. The addition of the additive to Surlyn[®] 8940 could contribute to the desirable properties of React-A-Seal[®] at elevated temperatures.

The creep recovery curves describe the response of the ionomers, after creeping, to lowering the stress to zero. The magnitude of the recoverable compliance for the React-A-Seal[®] is about half as large as the recoverable compliance of the Surlyn[®] 8940 and this observation could be due to the silicon-based additive in the React-A-Seal[®]. Despite this, all of the materials showed similar trends in their creep recovery response; at low temperatures more recovery was observed while at high temperatures much less recovery was noted. Also, note that none of the materials recovered to zero compliance. This observation indicated that permanent plastic deformation, also described as permanent “set”, occurred during the creeping of Nucrel[®] 925, Surlyn[®] 8940, React-A-Seal[®], and Surlyn[®] 8920 at 1.5 MPa stress.

High-impact applications do not depend on whether the ionomers show evidence of permanent plastic deformation. The “high-impact” feature of the applications requires that large stresses, much larger than 1.5 MPa, caused by the projectile energy transfer, be experienced by the ionomers. Due to this feature, linear viscoelastic behavior is not expected, so the recovery curve observations serve only as a guideline for comparisons of the EMAA samples.

Time-temperature superposition (tTSP) was performed using the creep curves (presented in Section 1.3.2). The reference temperature for the superpositions was 52°C. Two criteria must be met for a master curve to be used to predict material properties: 1) the master curve isotherms must overlap significantly and, 2) the shift factor plots must be smooth curves and have no discontinuities. These two criteria imply a single mechanism for the range of temperatures employed. Figures 4.6, 4.7, 4.8, and 4.9 show the master curves and shift factor plots for Nucrel[®] 925, Surlyn[®] 8940, React-A-Seal[®], and Surlyn[®] 8920, respectively.

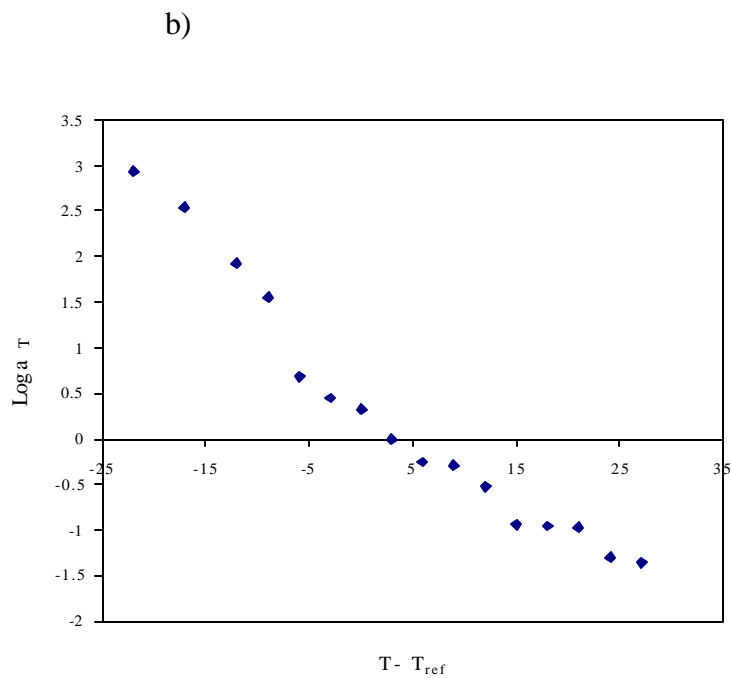
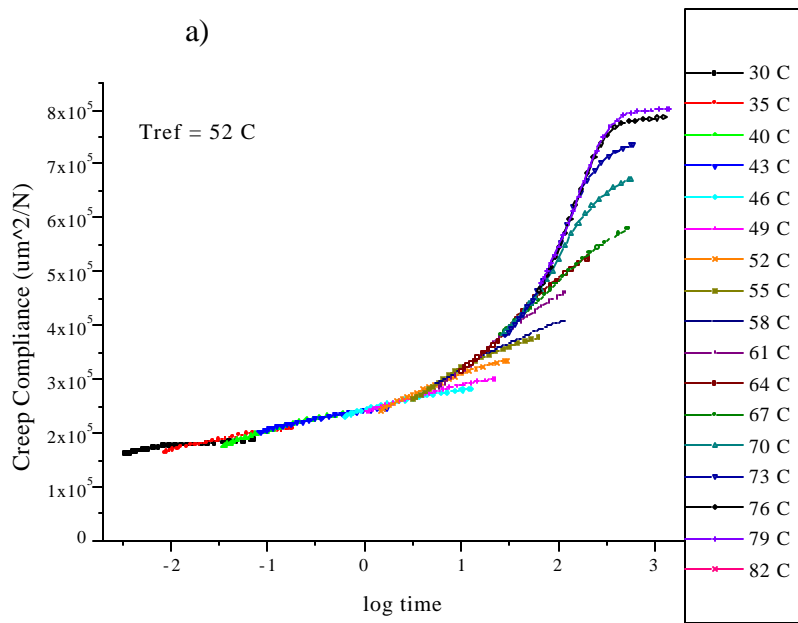


Figure 4.6. (a) tTSP master curve and (b) shift factor plot for Nucrel[®] 925

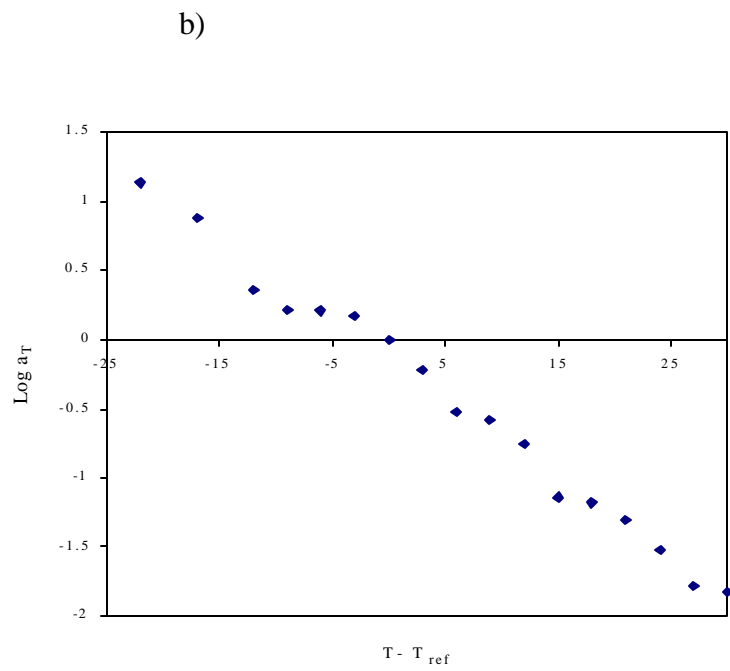
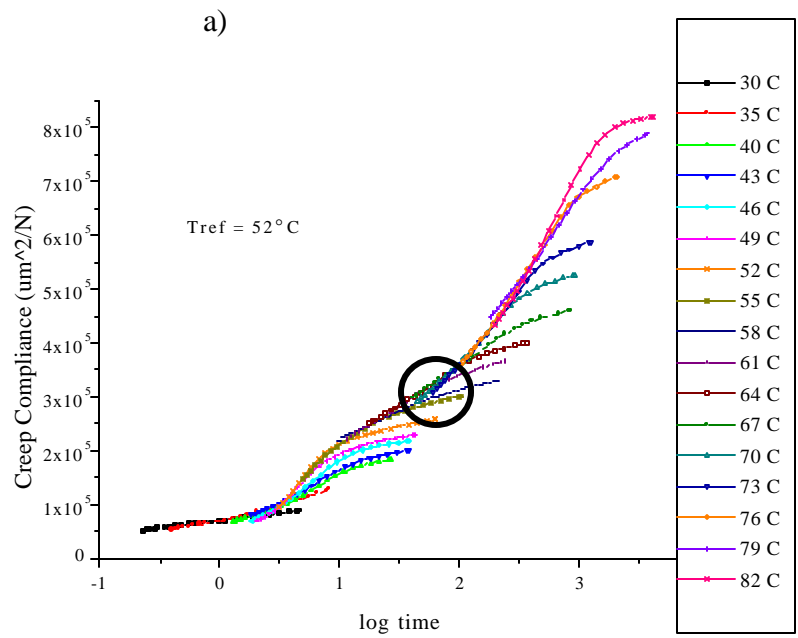


Figure 4.7. (a) tTSP master curve and (b) shift factor plot for Surlyn[®] 8940

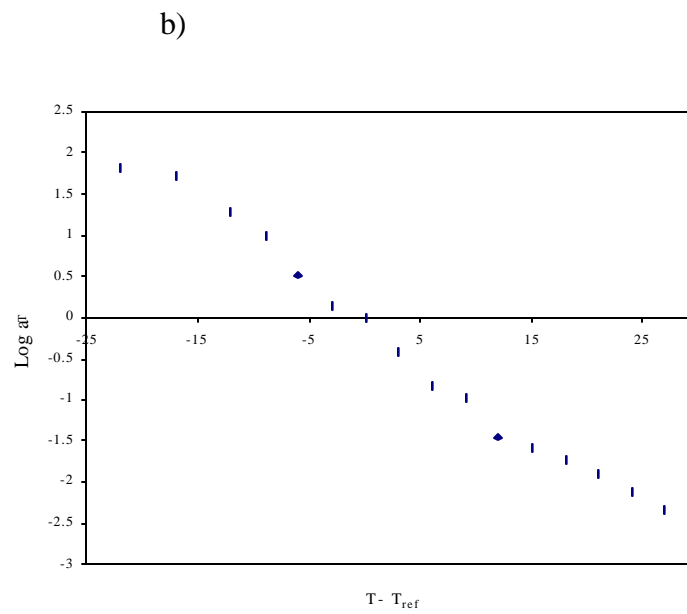
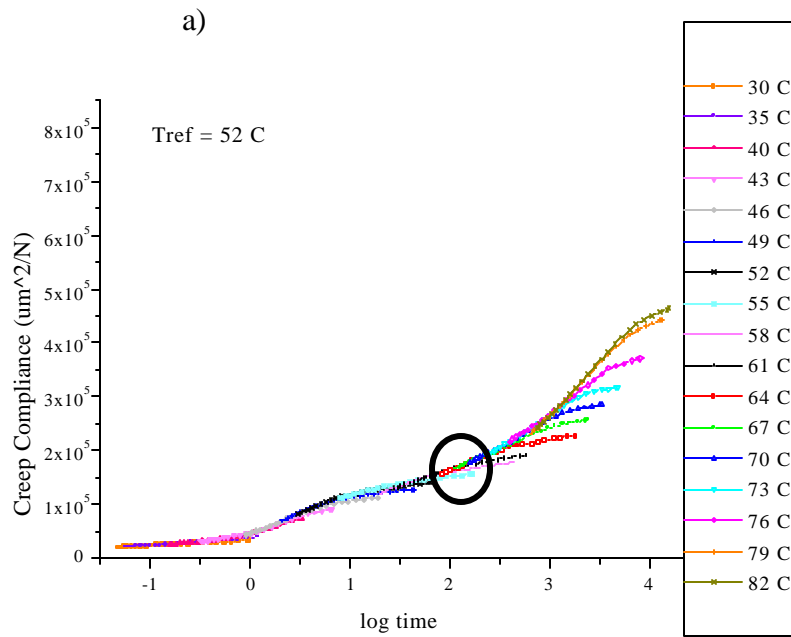
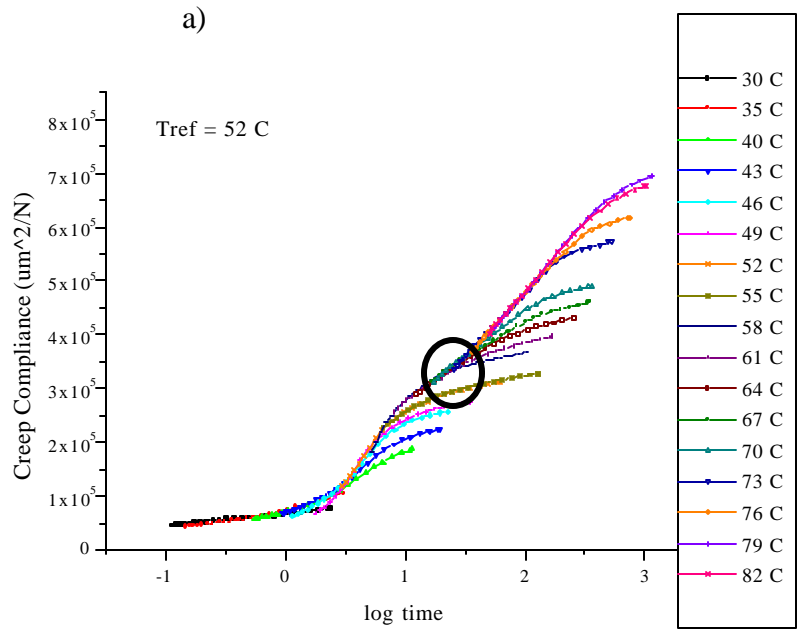


Figure 4.8. (a) tTSP master curve and (b) shift factor plot for React-A-Seal[®]



b)

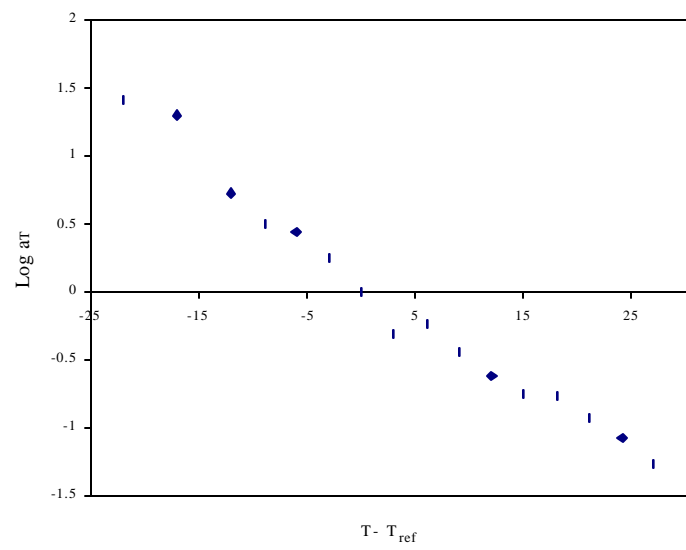


Figure 4.9. (a) tTSP master curve and (b) shift factor plot for Surlyn[®] 8920

A “tailing” effect of the creep isotherms is observed in the master curves. These tails deviate from the master curve and are likely due to structural changes, like the level of crystallinity, in these ionomers with temperature. A proposed structural change will be discussed in the next section. Despite this tailing, all of the ionomer isotherms superimposed well, as can be seen from the shift factor plots. Nucrel[®] 925 showed a uniformly smooth master curve. However, Surlyn[®] 8940, React-A-Seal[®], and Surlyn[®] 8920 did not show uniformly smooth master curves. The Surlyn[®] 8940, React-A-Seal[®], and Surlyn[®] 8920 master curves exhibited a change in slope of the creep isotherms with superposition around 55°C (outlined in black in Figures 4.7, 4.8, and 4.9) signifying a change in mechanism in the master curves. This change in mechanism is synonymous with a change in at least one of the polymer parameters of the ionomers. These experimental creep temperatures are very close to the temperatures at which the order-disorder transition occurred in the DSC and DMA experiments. Table 4.1 shows a comparison of the order-disorder transition temperatures from the DSC, DMA frequency dependent data, and the DMA creep data.

Table 4.1

Comparison of the order-disorder transition temperatures from the DSC, DMA frequency dependent data, and the DMA creep data

Sample	DSC T _i	T _i of α' peak at 10 Hz	Temperature of Slope Change in the Creep Data
Nucrel [®] 925	52.5°C	-	-
Surlyn [®] 8940	51.9°C	50.2°C	55°C
React-A-Seal [®]	52.2°C	50.3°C	55°C
Surlyn [®] 8920	52.6°C	59.3°C	58°C

The temperatures of the slope changes are slightly higher than the temperatures of the order-disorder transition obtained from the DSC and DMA frequency dependent data. However, considering the difference in the measuring techniques, the temperature difference was not

significant and so this change in mechanism was attributed to the ordering and disordering of the ionic aggregates.

At temperatures near the order-disorder transition and higher, the creep isotherms of Nucrel[®] 925, Surlyn[®] 8940, React-A-Seal[®], and Surlyn[®] 8920 could not be reproduced. To elucidate the reason for the irreproducibility, physical aging experiments were performed using DSC.

4.1.1. DSC - Aging

Figures 4.10, 4.11, 4.12, and 4.13 show 30-minute aging curves of Nucrel[®] 925, Surlyn[®] 8940, React-A-Seal[®], and Surlyn[®] 8920, respectively, at various aging temperatures in nitrogen.

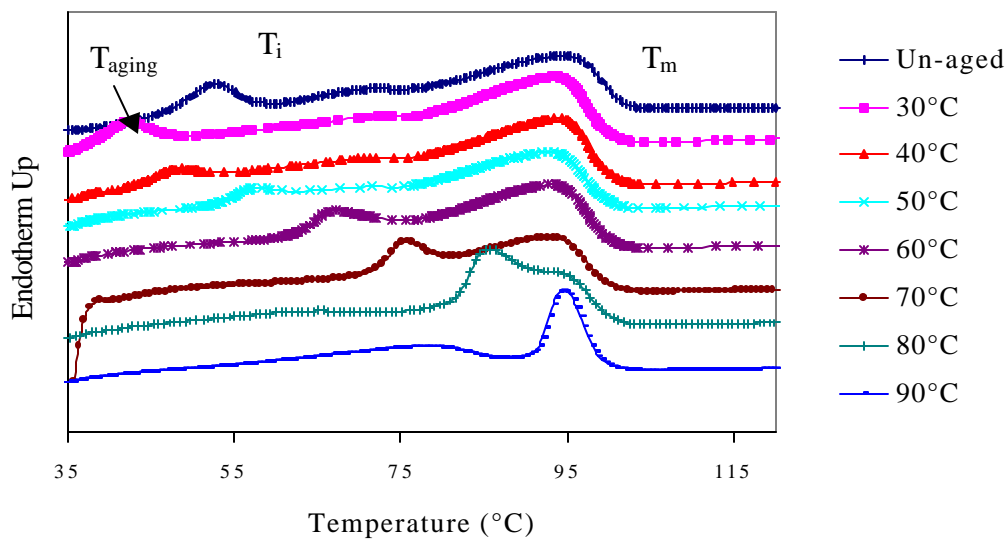


Figure 4.10. Aging of Nucrel[®] 925 for 30 minutes in the DSC from 30°C to 90°C

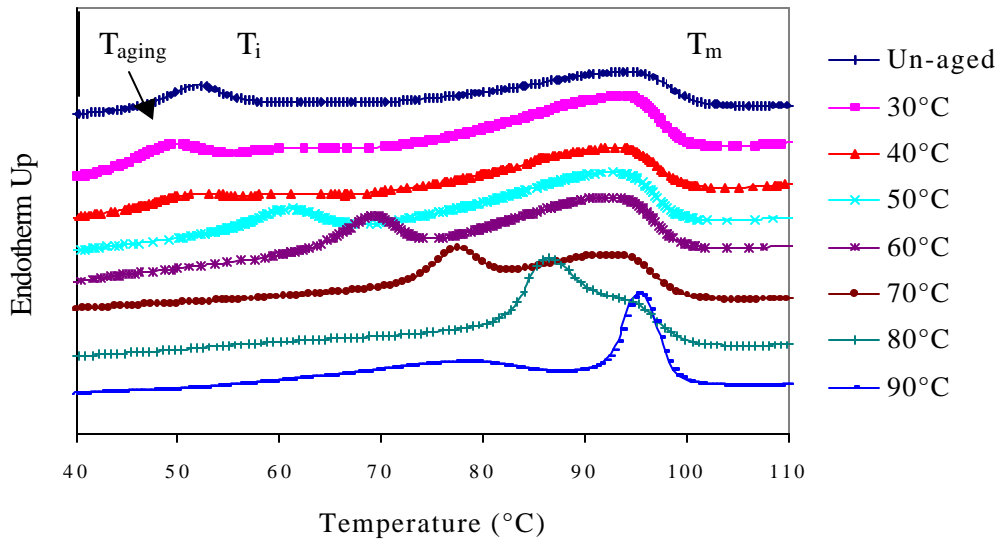


Figure 4.11. Aging of Surlyn[®] 8940 for 30 minutes in the DSC from 30°C to 90°C

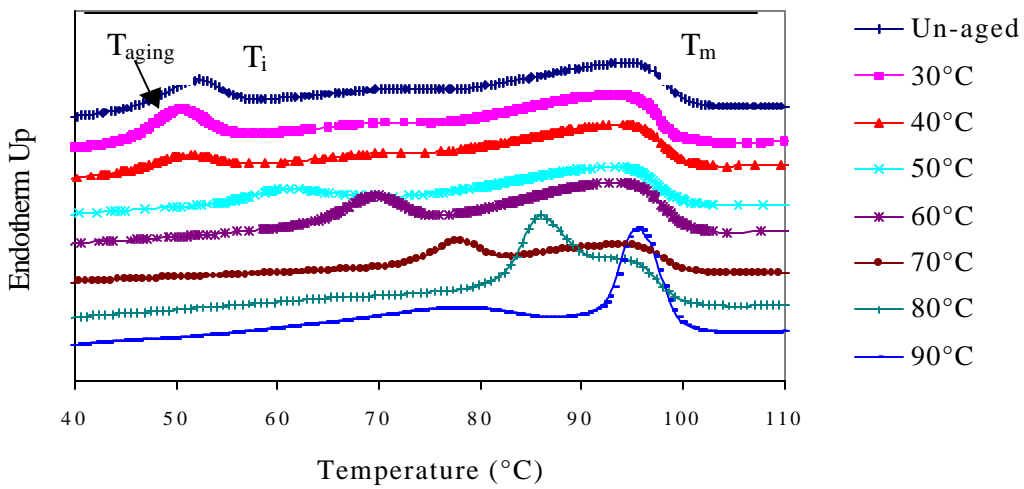


Figure 4.12. Aging of React-A-Seal[®] for 30 minutes in the DSC from 30°C to 90°C

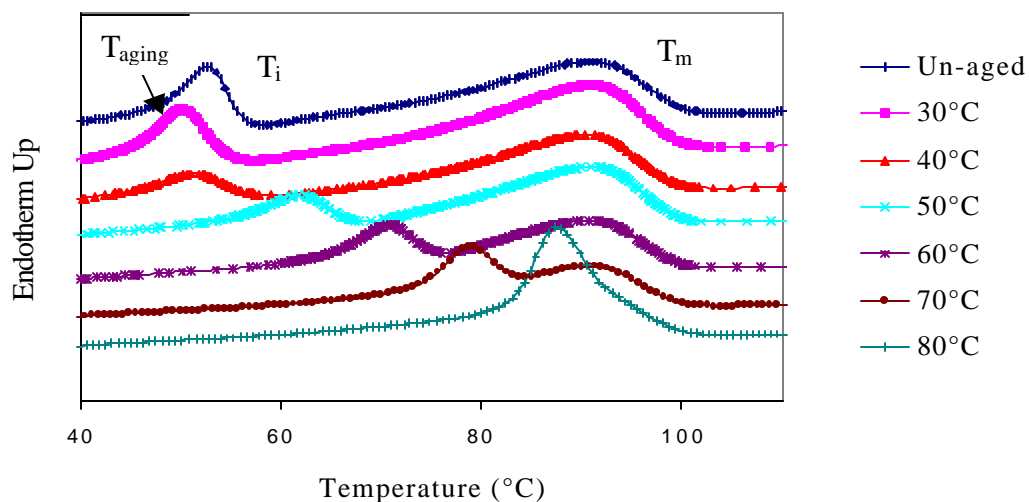


Figure 4.13. Aging of Surlyn[®] 8920 for 30 minutes in the DSC from 30°C to 80°C

The first heating cycle, from 30°C to 150°C at 5°C/minute, was applied to the un-aged samples. These un-aged heating curves for Nucrel[®] 925, Surlyn[®] 8940, React-A-Seal[®], and Surlyn[®] 8920 showed two transitions. As previously labeled in Section 3.3, the lower temperature peak (~50°C) was ascribed to the order-disorder transition of the ionic and polar aggregates, and the upper temperature peak (~95°C) signified the melting of the polyethylene crystals. Upon completion of the first heating cycle, both the ionic and polar aggregates were disordered, as already discussed in Section 3.3.

All the samples, following the first heating cycle, were aged in the DSC furnace for 30, 60, 90, and 120 minutes at 30, 40, 50, 60, 70, 80, and 90°C. Then heating cycles were performed after each aging time (at each aging temperature) from 30°C to 150°C at 5°C/minute. The aged samples for Nucrel[®] 925, Surlyn[®] 8940, React-A-Seal[®], and Surlyn[®] 8920 also showed two transitions. Due to the disordered state of the aggregates prior to the aging study, the lower temperature peak, which shifts with aging temperature, cannot be attributed to the order-disorder transition. According to Tadano *et al.*¹, this new aging peak might result from the melting of so-called quasi-crystallites in the polyethylene regions. The higher temperature peak (~95°C) was attributed to the melting of the polyethylene crystallites.

Table 4.2 shows the peak maximum and percent crystallinities as a function of aging time and temperature for each sample. The percent crystallinity was calculated assuming that the heat of fusion² of the polyethylene crystallites is 290.4 J/g.

Table 4.2

Comparison of the peak maximum and percent crystallinity for the quasi-crystalline peak for each sample and percent crystallinity for the melting peak for each sample

	Quasi-Crystalline Peak		Melting Peak
	Peak Maximum	% Crystallinity	% Crystallinity
Nucrel^O 925 – 30° C			
60 minutes	39.02°C	0.5036	16.5
120 minutes	39.08°C	0.5354	16.29
Nucrel^O 925 – 50° C			
60 minutes	57.63°C	0.7775	11.13
120 minutes	58.47°C	1.287	10.09
Nucrel^O 925 – 90° C			
30 minutes	-	-	14.52
60 minutes	-	-	15.85
Surlyn^O 8940 – 30° C			
60 minutes	44.2°C	0.8994	10.89
120 minutes	44.91°C	1.209	11.33
Surlyn^O 8940 – 50° C			
60 minutes	61.3°C	2.397	9.989
120 minutes	62.35°C	2.864	10.43
Surlyn^O 8940 – 90° C			
60 minutes	-	-	14.75
120 minutes	-	-	15.08

	Quasi-Crystalline Peak		Melting Peak
	Peak Maximum	% Crystallinity	% Crystallinity
React-A-Seal[®] – 30° C			
60 minutes	43.66°C	0.7213	13.14
120 minutes	45.18°C	0.9122	12.56
React-A-Seal[®] – 50° C			
60 minutes	61.07°C	2.386	10.96
120 minutes	62.17°C	2.796	10.87
React-A-Seal[®] – 90° C			
30 minutes	-	-	16.51
60 minutes	-	-	15.73
Surlyn[®] 8920 – 30° C			
60 minutes	45.42°C	1.473	13.39
120 minutes	46.89°C	2.031	12.75
Surlyn[®] 8920 – 50° C			
60 minutes	63.38°C	3.385	10.29
120 minutes	64.71°C	3.899	9.953
Surlyn[®] 8920 – 90° C			
30 minutes	-	-	13.52
60 minutes	-	-	13.6

With increased aging time and annealing temperature Nucrel[®] 925, React-A-Seal[®], and Surlyn[®] 8920 all showed a shift of the quasi-crystalline peak to higher temperatures, an increase in the percent crystallinity of the quasi-crystalline peak, and a decrease in the percent crystallinity of the melting peak. Surlyn[®] 8940 showed the same trends except there were no significant changes in the percent crystallinity of the melting peak. At ~50°C the quasi-

crystalline peak and the melting peak began to converge. At 90°C they joined into one melting peak for the Nucrel[®] 925, React-A-Seal[®], and Surlyn[®] 8940. For the Surlyn[®] 8920 the peak merges at 80°C. For each ionomer the percent crystallinity of the new melting peak increased by ~5%.

4.2. Summary

The aging of Nucrel[®] 925, Surlyn[®] 8940, React-A-Seal[®], and Surlyn[®] 8920, as a function of time and temperature, helped in interpreting the irreproducibility of the creep and creep recovery curves which had produced “tailing” in the creep isotherms. As already established by Tadano *et al.*¹ using similar EMAA ionomers, increased aging time and temperature consequently caused changes in the polyethylene matrix which led to complexities in crystallinity. As the samples creep or creep recover with time at each isotherm, aging also occurred, and the magnitude and shape of the resulting curves depended on changes in the crystalline morphology of the polyethylene matrix. These changes could include differences in the rate of crystallization and variation in the initial amount of crystallization among samples.

It was unexpected that the aging resulted from changes in the polyethylene matrix. Traditional physical aging can only occur below the glass transition temperature and the T_g of the polyethylene matrix is around -120°C³. The temperature of the storing conditions and temperature of the experimental conditions for the creep and creep recovery experiments were much higher than -120°C. However, in these materials it is suggested that the aging is due to changes in the ionic aggregates and surrounding matrix since the creep and creep recovery experiments began below the T_i , the glass transition of the ionic clusters. Crystallization of the polyethylene matrix with aging time and temperature made it difficult to reproduce the creep and creep recovery data.

4.3. References

1. Tadano, K.; Hirasawa, E.; Yamamoto, H.; Yano, S. *Macromolecules* **1989**, *22*, 226-233.
2. Kutsumizu, S.; Tadano, K.; Matsuda, Y.; Goto, M.; Tachino, H.; Hara, H.; Hirasawa, E.; Tagawa, H.; Muroga, Y.; Yano, S. *Macromolecules* **2000**, *33*, 9044-9053.

3. McCrum, N.G.; Read, B.E.; Williams, G.W. *Anelastic and Dielectric Effects in Polymeric Solids*. Dover Publications, Inc. New York, 1967.

5.Results and Discussion

High-Speed Impact Projectile Testing

The thermodynamic and viscoelastic experiments described thus far have established a correlation between the data presented here and in the literature; there has been little mention of how they relate to the self-healing phenomenon.

It is believed that the self-healing phenomenon is related to the ionic aggregation and its effect on the properties of EMAA and EMAA ionomers. It is the aim of this chapter to present a possible relationship between the self-healing phenomenon and the thermodynamic and viscoelastic properties of the ionomers.

5.1. Pistol Range

The ~2 mm thick samples of Surlyn[®] 8940 (EMAA-0.30Na), React-A-Seal[®] (based on EMAA-0.30Na), and Surlyn[®] 8920 (EMAA-0.60Na) all self-healed upon high-speed impact with a 9-mm bullet at the tested velocities. None of the samples self-healed upon high-speed impact with the 9-mm blunt ended cylindrical bullet. The blunt-ended cylindrical bullet acted as a “cookie cutter”, removing the material in its path, whereas the standard 9-mm bullet compressed the material to the side. Figure 5.1 shows an example of a healed hole (pointed out by blue arrows) and an un-healed hole (pointed out by blue hash marks), both pictured from the point of entry.

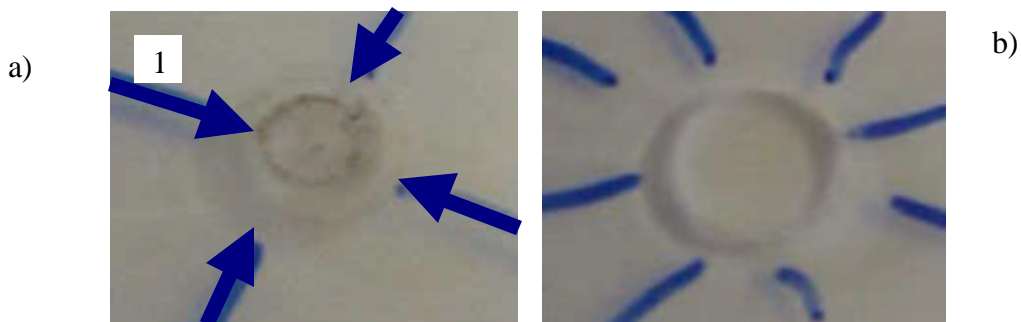


Figure 5.1. Sample of React-A-Seal[®] (a) healed after high-speed impact with standard 9mm bullet, (b) un-healed after high-speed impact with the blunt-ended cylindrical bullet

The small ring of dark coloring (pointed out by blue arrow 1) in the healed portion of the material was due to residue from the bullet and was observed for the EMAA samples. Surlyn[®] 8940 and React-A-Seal[®] both showed a small dimple at the bullet entry point and a small trail of material protruding from the bullet exiting point after healing. Surlyn[®] 8920 showed the same healing characteristics as the Surlyn[®] 8940 and React-A-Seal[®] except that a radial “cracking” pattern was observed in the healed portion of the material. Water was placed on the healed material and no leaking was observed, indicating that the ionomers fully self-healed.

The Nucrel[®] 925 also did not heal upon impact with the 9-mm blunt-ended cylindrical bullet. Unexpectedly, Nucrel[®] 925 (EMAA) did self-heal upon impact with the 9-mm bullets at the tested velocities and had the same healing characteristics as the Surlyn[®] 8940 and React-A-Seal[®]. The healing of Nucrel[®] 925 was unexpected because it was originally thought that the self-healing phenomenon was due to the ionic character alone. It was originally theorized that healing would occur if an adequate amount of energy, whether heat energy, elastic stored energy, or electrostatically stored energy, could be transferred to the ionomer thereby causing the temperature of the ionic material to increase through the order-disorder transition. It could be explained then that with impact from a bullet, heat energy was transferred to the ionomer thereby causing the temperature increase and disordering of the ionic aggregates. With the removal of the heat energy, the bullet exiting the ionomer, the ionic aggregates re-ordered causing the ionomer to heal. The fundamentals of this theory are schematically shown in Figure 5.2.

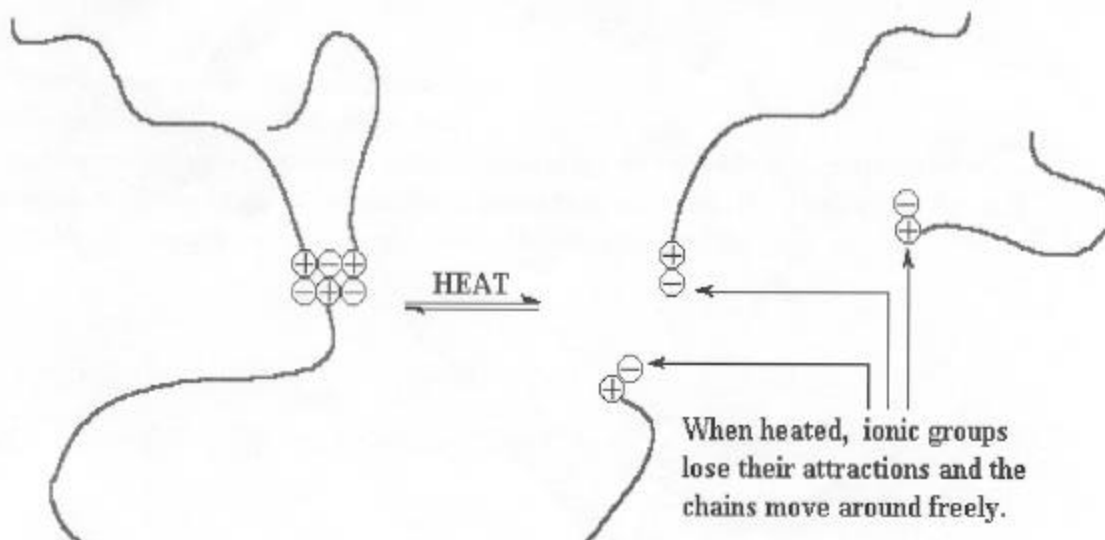


Figure 5.2. Schematic showing the ordering and disordering of an ionic aggregate with heat as the source of energy³

A healing theory in which a temperature increase (alone) taking the polymers through its order-disorder transition is not supported considering that Nucrel[®] 925 contains no ionic character and only weakly aggregated polar character. A thermal IR camera was used to more carefully investigate the temperature increase with heat transfer from the bullet.

5.1.1. Thermal IR Camera

The thermal IR camera was able to capture the ambient temperature of the samples before bullet penetration and the resulting temperature of the samples after bullet penetration. Figure 5.3 shows one example of a thermal IR image.

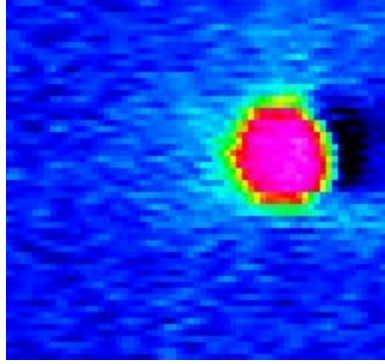


Figure 5.3. A thermal IR image from React-A-Seal[®]. The blue represents ambient temperature (~28°C). The dark pink (~98°C) represents the point of bullet penetration. The colors radiating out from the dark pink represent the dissipation of heat from the point of entry.

Table 5.1 lists thermal and impact data for React-A-Seal[®]. The React-A-Seal[®] thermal data is nearly identical to the thermal data for Nucrel[®] 925, Surlyn[®] 8940, and Surlyn[®] 8920. Also, the velocity change for Nucrel[®] 925, Surlyn[®] 8940, and Surlyn[®] 8920 follows the same trend as the bullet velocity change for React-A-Seal[®].

Table 5.1

Data for React-A-Seal[®] showing the changes in temperature of the sample with impact of a 9-mm bullet and the changes in velocity of the bullet upon impact

Initial Bullet Velocity - Before Penetration	1156 ft/s	589 ft/s	404 ft/s
Final Bullet Velocity - After Penetration	1135 ft/s	553 ft/s	344 ft/s
Δ Velocity	21 ft/s	36 ft/s	60 ft/s
Ambient Temperature	28.3°C	28.3°C	28.3°C
Temperature After Penetration	98.1°C	98.3°C	98.1°C
Δ Temperature	69.8°C	70°C	69.8°C

Table 5.1 shows that with each decrease in initial bullet velocity, the change in velocity with impact significantly increased. This increase in velocity change should translate into more

energy loss of the bullet, resulting in more energy absorbed by the sample, and finally resulting in an increase in sample temperature. However, this postulated increase in the sample temperature with larger decrease in bullet velocity was not observed. Nucrel[®] 925, Surlyn[®] 8940, React-A-Seal[®], and Surlyn[®] 8920 all showed the same magnitude of temperature change despite the changes in velocity of the bullet. All of the samples exhibited a temperature of ~98°C after penetration and required ~3 minutes to cool to ambient temperature (28°C). The temperature reached by Nucrel[®] 925, Surlyn[®] 8940, React-A-Seal[®], and Surlyn[®] 8920 was above their melting temperature as measured by DSC (~95°C). It was speculated, because of this observation that viscosity effects aided in the self-healing phenomenon. Therefore, a rheometer was used to investigate the viscosity of these EMAA samples at several temperatures.

5.1.2. Rheometer

Recall that a rheometer measures the melt flow deformation properties, such as viscosity, of a material. It is known^{1,2} that ionic character in a polymer increases the viscosity of that polymer by orders of magnitude. Figure 5.4 is a plot of viscosity as a function of shear rate at 90, 110, 130, and 150°C for Nucrel[®] 925, Surlyn[®] 8940, React-A-Seal[®], and Surlyn[®] 8920.

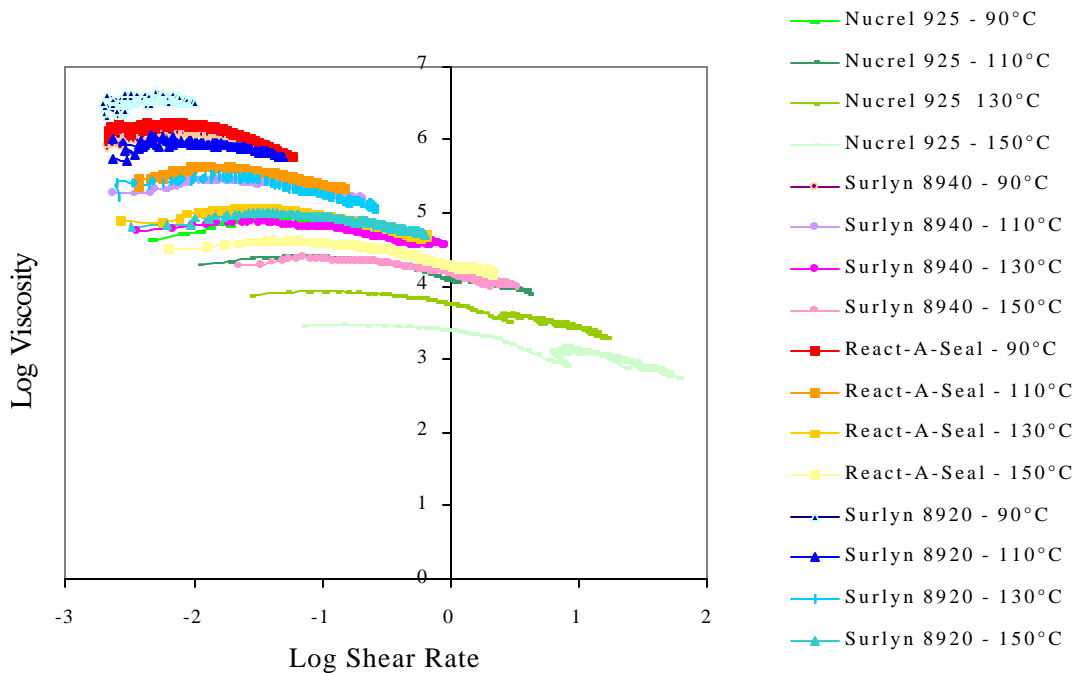


Figure 5.4. Graph of viscosity as a function of shear rate for Nucrel[®] 925, Surlyn[®] 8940, React-A-Seal[®], and Surlyn[®] 8920 at 90, 110, 130, and 150°C

As the ionic content decreased in the EMAA ionomers, the viscosity decreased. This trend in viscosity can be more clearly examined in Table 5.2.

Table 5.2
Apparent viscosities reached at the maximum stresses

	Temperatures Measured				units
	90°C	110°C	130°C	150°C	
Nucrel [®] 925	$3.8 \cdot 10^4$	$8.5 \cdot 10^3$	$2.1 \cdot 10^3$	$5.6 \cdot 10^2$	Pa-s
Surlyn [®] 8940	$8.5 \cdot 10^5$	$1.6 \cdot 10^5$	$3.6 \cdot 10^4$	$9.7 \cdot 10^3$	Pa-s
React-A-Seal [®]	$5.6 \cdot 10^5$	$2.2 \cdot 10^5$	$5.1 \cdot 10^4$	$1.7 \cdot 10^4$	Pa-s
Surlyn [®] 8920	$3.2 \cdot 10^6$	$5.2 \cdot 10^5$	$1.3 \cdot 10^5$	$5.1 \cdot 10^4$	Pa-s

The Nucrel[®] 925, with no ionic character, flowed the most while the Surlyn[®] 8920, with the most ionic character, flowed the least with the applied stress; Surlyn[®] 8920 is very viscous. The Surlyn[®] 8940 flowed more than the React-A-Seal[®], especially at higher temperatures. Perhaps the presence of the chemically bonded silicon (as detected by the XPS) in the React-A-Seal[®] contributed to its more viscous behavior.

The rheometer could not apply a stress comparable to the stress applied by a high-speed impact bullet. Therefore, in spite of the trends observed in the viscosity data, there were no conclusions possible on the contribution of the viscosity to healing of the EMAA ionomers upon high-speed impact.

5.2. References

1. Vanhoorne, P.; Register, R. A. *Macromolecules* **1996**, *29*, 598-604.
2. Kang, K.K.; Jeong, Y-E.; Lee, D-H.; Shiono, T.; Ikeda, T. *J. Macromol. Sci.—Phys.* **1999**, *3*, 227-236.
3. <http://babylon.u-3mrs.fr:10085/~www-pol/ionomer.html>

6. Comments on the Self-Healing Phenomenon

The research in this study suggested that ionic aggregation and melt flow behavior are two characteristics that contribute to the self-healing ability of Nucrel[®] 925, Surlyn[®] 8940, React-A-Seal[®], and Surlyn[®] 8920.

Nucrel[®] 925 (EMAA) exhibited weak aggregation, possibly due to intermolecular and intramolecular attraction of the polar carboxyl groups. Aggregation was inferred from the presence of an order-disorder transition measured in the DSC. However, the order-disorder transition was not detected in the dynamic or viscoelastic experiments, hence the proposal of weak aggregation.

Surlyn[®] 8940 (EMAA-0.30Na), React-A-Seal[®] (based on EMMA-0.30Na), and Surlyn[®] 8920 (EMAA-0.60Na) displayed stronger aggregation due to increased ionic interactions with increased sodium neutralization. These EMMA ionomers exhibited an order-disorder transition in the DSC, the dynamic, and the viscoelastic experiments.

The thermal IR images captured during the high-speed bullet impact testing showed a uniform increase in the temperature of the EMMA samples to $\sim 5^{\circ}\text{C}$ above their melting temperatures ($\sim 95^{\circ}\text{C}$) following impact. The large temperature increase, 70°C above ambient temperature, caused by the impact suggested that melt flow properties were contributing to self-healing.

The melt flow properties were measured using a rheometer. Nucrel[®] 925, Surlyn[®] 8940, React-A-Seal[®], and Surlyn[®] 8920 exhibited viscosities on the order of $\sim 10^4 - 10^6$ Pa-s at temperatures between 90°C to 150°C . This increased viscosity, compared to polyethylene (~ 23 Pa-s), was speculated to be a direct result of aggregation, especially ionic aggregation.

Together, the high viscosity and the resistance to motion of the aggregates raise the amount of energy absorbed by the EMMA samples upon high-speed impact. EMMA samples seem to self-heal if enough energy is transferred from the projectile to the sample to cause a temperature increase above the melting temperature. The increased elastic character of the melt, due to viscosity, primarily drives the healing phenomenon.

7. Future Work

Additional experiments are essential for continued clarification of the polymer and ionomer characteristics required for self-healing.

To better understand the unexpected healing of Nucrel[®] 925, other polymers, for example nitriles, amides, urethanes, and carbonates with stronger intermolecular and intramolecular forces could be studied under high-speed impact. The puncture reversibility or irreversibility of these materials would elucidate the importance of intermolecular and intramolecular aggregation.

The aged samples (annealed) could be shot under high-speed impact to learn more about the healing of the EMAA ionomers. This experiment would provide information on the effect of increased crystallinity on healing. Also, due to the disordered state of the ionomers during aging, if healing still occurred with high-speed impact, perhaps then ionic aggregation does not aid in healing. Testing of other ionomers with varying types and concentrations of cations could be performed if it is determined that aggregation is in fact necessary for healing.

It is also important to continue understanding how aggregation and flow behavior alter the thermal, physical, and mechanical behaviors of polymers and ionomers. A threshold velocity could be observed for healing if a method were developed to vary the velocity of a projectile. This threshold velocity could then be converted into energy and possibly correlated to the amount of energy needed to overcome thermal and mechanical transitions as measured in the DSC or DMA.

In addition, to better understand the elastic melt flow behavior of these EMAA materials, the melt elasticity could be measured.

Finally, a high-speed camera that captures images at more than 10,000 frames per second could be used to visually observe the healing phenomenon. With this visual observation, perhaps the elastic behavior, due to the high viscosity of the ionomers or polymers could be investigated.

Vita

Rebecca Fall was born to Alan and Rachel Fall on May 14, 1978 in Rochester, New Hampshire. She has a younger brother, Ethan, and a younger sister, Melissa. Rebecca grew up on a farm in Freedom, New Hampshire. After graduating from Kennett High School in 1996, Rebecca attended college at Virginia Tech. During her sophomore year in the Corps of Cadets, Rebecca and John, a fellow cadet, met and fell in love. She graduated in May 2000 with her Bachelor of Arts degree in Chemistry and proceeded to immediately begin her masters degree. Rebecca defended her Masters of Science Thesis in Chemistry on August 29, 2001. Rebecca is moving to Virginia Beach to be with John and working for a company in the Tidewater area.